

# Tectonics

## RESEARCH ARTICLE

10.1029/2020TC006331

### Key Points:

- Deposition of the 130 and 100 Ma Newark Canyon Formation was related to low-magnitude shortening in the Sevier hinterland
- Late Jurassic shortening in the Sevier hinterland coincided with eastward migration of the basal Sevier décollement
- Between ~130 and 75 Ma, shortening was partitioned between the Sevier fold-thrust belt and the Sevier hinterland

### Supporting Information:

Supporting Information may be found in the online version of this article.

### Correspondence to:

R. V. Di Fiori,  
[russellid@uidaho.edu](mailto:russellid@uidaho.edu)

### Citation:

Di Fiori, R. V., Long, S. P., Fetrow, A. C., Snell, K. E., Bonde, J. W., & Vervoort, J. D. (2021). The role of shortening in the Sevier hinterland within the U.S. Cordilleran retroarc thrust system: Insights from the cretaceous Newark canyon formation in central Nevada. *Tectonics*, 40, e2020TC006331. <https://doi.org/10.1029/2020TC006331>

Received 23 MAY 2020

Accepted 27 APR 2021

## The Role of Shortening in the Sevier Hinterland Within the U.S. Cordilleran Retroarc Thrust System: Insights From the Cretaceous Newark Canyon Formation in Central Nevada

Russell V. Di Fiori<sup>1,2</sup> , Sean P. Long<sup>1</sup> , Anne C. Fetrow<sup>3</sup> , Kathryn E. Snell<sup>3</sup> , Joshua W. Bonde<sup>4</sup> , and Jeff D. Vervoort<sup>2</sup>

<sup>1</sup>School of the Environment, Washington State University, Pullman, WA, USA, <sup>2</sup>Idaho Geological Survey, Morrill Hall, University of Idaho, Moscow, ID, USA, <sup>3</sup>Department of Geological Sciences, University of Colorado Boulder, Boulder, CO, USA, <sup>4</sup>Las Vegas Natural History Museum, Las Vegas, NV, USA

**Abstract** Documenting the spatio-temporal progression of deformation within fold-thrust belts is critical for understanding orogen dynamics. In the North American Cordillera, the geometry, magnitude, and timing of contractional deformation across a broad region of Nevada known as the “Sevier hinterland” has been difficult to characterize due to minimal exposures of syn-contractional sedimentary rocks and overprinting of Cenozoic extension. To address this, we present geologic mapping and U-Pb zircon geochronology from three exposures of the Cretaceous Newark Canyon Formation (NCF) in central Nevada. In the Cortez Mountains, NCF deposition between ~119 and 110 Ma is hypothesized to be related to generation of relief by thrusting/folding to the west. In the Fish Creek Range, NCF deposition between ~130 and 100 Ma was related to motion on an east-vergent thrust fault. In the Pancake Range, NCF deposition is bracketed between ~129 and 66 Ma and post-dated east-vergent folding. We incorporate these timing constraints into a compilation of deformation timing in the Sevier hinterland. Late Jurassic (~165 and 155 Ma) shortening, which is largely post-dated shortening in the Luning-Fencemaker thrust belt to the west and pre-dated initial deformation in the Sevier fold-thrust belt to the east, is interpreted to represent diffuse, low-magnitude deformation that accompanied eastward propagation of the basal Cordilleran décollement. Cretaceous (~130 and 75 Ma) hinterland shortening, which includes deformation associated with NCF deposition, was contemporaneous with shortening in the Sevier fold-thrust belt. This is interpreted to represent long-duration strain partitioning between the foreland and hinterland during continued coupling above the basal décollement and the progressive westward underthrusting of thick North American lower-middle crust.

## 1. Introduction

Documenting the space-time evolution of deformation within fold-thrust belts is fundamental for understanding the dynamics of orogenesis. However, gleaning the history of shortening within fold-thrust belts is often a difficult task, as thrust systems do not always propagate in-sequence, deformation geometry and style can vary significantly both along-strike and across-strike, and preserved field relations often only allow for broad bracketing of the timing of thrusting and folding events (e.g., Chapple, 1978; Diegel, 1986; McQuarrie & DeCelles, 2001; Morley, 1988). The Western U.S. portion of the North American Cordilleran orogen (Figure 1), which experienced a ~100 Myr history of contractional deformation between the Jurassic and the Paleogene, exemplifies all of these challenges, and is also complexly overprinted by Cenozoic extensional tectonism that formed the Basin and Range Province (e.g., Allmendinger, 1992; Burchfiel et al., 1992; Dickinson, 2004; Wernicke, 1992; Yonkee & Weil, 2015). The majority of crustal shortening (~200 km) during the construction of the Cordillera was accommodated in the Sevier fold-thrust belt in western Utah and southern Nevada (Figure 1), where decades of investigations have yielded a solid understanding of thrust geometry, kinematics, and timing (e.g., Allmendinger et al., 1987; Armstrong, 1968; DeCelles, 2004; DeCelles & Coogan, 2006; Royse et al., 1975; Villien & Kligfield, 1986; Yonkee et al., 2019; Yonkee & Weil, 2015). However, to the west of the Sevier fold-thrust belt, in the interior of the retroarc region in eastern and central Nevada, which is often referred to as the “Sevier hinterland” (Figure 1) (e.g., Armstrong, 1972), many uncertainties remain regarding the spatial extent, geometry, style, timing, and magnitude of Cordilleran shorten-

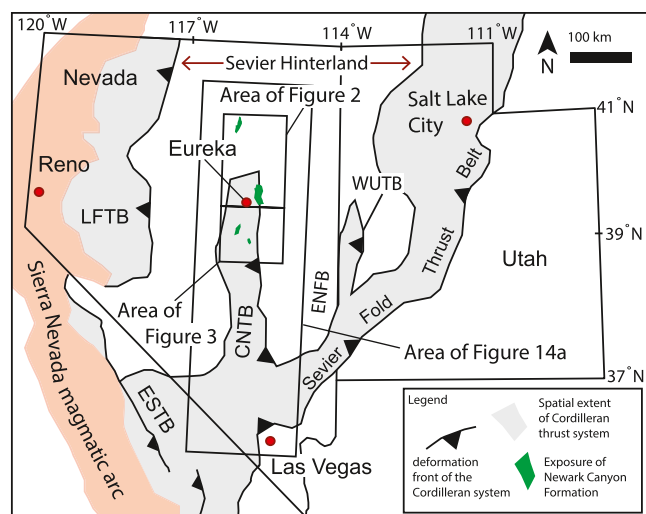


**Figure 1.** Map showing Cordilleran thrust systems of Nevada and Utah (modified from Long, Henry, Muntean, Edmondo, & Cassel, 2014). The approximate spatial extents of Cordilleran thrust systems are shaded and the Sierra Nevada magmatic arc is shown in red. Exposures of the Cretaceous Newark Canyon Formation are shown in green. ENFB, Eastern Nevada fold belt; WUTB, western Utah thrust belt.

ing (e.g., Gans & Miller, 1983; Greene, 2014; Long & Walker, 2015; Speed et al., 1988; Taylor et al., 2000). These uncertainties can be largely attributed to the complex overprint of Cenozoic extension (Dickinson, 2004; Gans & Miller, 1983), widespread cover under Paleogene volcanic deposits (Henry & John, 2013), Late Cretaceous metamorphism that has overprinted older metamorphism within core complexes (Hodges et al., 1992; Miller et al., 1988), and the scarcity of Jurassic-Cretaceous, syn-orogenic sedimentary rocks across the hinterland region (Stewart, 1980).

Despite these challenges, researchers have defined upper-crustal Cordilleran structural provinces within the Sevier hinterland, including the central Nevada thrust belt (CNTB; Taylor et al., 2000), eastern Nevada fold belt (Long & Walker, 2015), and western Utah thrust belt (Greene, 2014) (Figure 1). Though progress has been made in understanding the geometry, style, and in some cases magnitude of deformation in these provinces, the largest challenge has proven to be precisely dating motion on thrust faults and growth of folds, which hinders placing deformation in the Sevier hinterland into the larger spatio-temporal framework of deformation in other portions of the Cordillera to the east and west.

In this study, we focus on the CNTB, which is defined as a system of north-striking, east-vergent thrust faults and folds that branches northward off of the Sevier fold-thrust belt in southern Nevada (Figure 1) (Di Fiori et al., 2020; Long, 2012; Long, Henry, Muntean, Edmondo, & Cassel, 2014; Long & Walker, 2015; Taylor et al., 1993; Taylor et al., 2000).

Based on cross-cutting relationships, deformation in most places in the CNTB can only be broadly bracketed between the Pennsylvanian-Permian and the Eocene (Nolan, 1962; Taylor et al., 1993; Taylor et al., 2000; Vandervoort & Schmitt, 1990). However, in the northern part of the CNTB and proximal areas to the north, isolated exposures of the Cretaceous Newark Canyon Formation (NCF), a terrestrial sedimentary unit that has long been postulated to have been deposited during regional contractional deformation (e.g., Di Fiori et al., 2020; Druschke et al., 2011; Nolan et al., 1974; Speed, 1983; Speed et al., 1988; Taylor et al., 2000), offer the opportunity to more narrowly bracket the timing of CNTB deformation.

In order to elucidate the depositional and deformational history of the NCF and how it relates to contractional deformation in the CNTB, we present new geologic mapping, stratigraphic divisions, U-Pb zircon geochronology, and conglomerate clast compositions from three map areas that contain exposures of the NCF, including the Cortez Mountains (Figure 2), the southern Fish Creek Range (Figure 3), and the central Pancake Range (Figure 3). The primary goal of our study is to explore the implications of our new age control and field relationships for the NCF on the geometry, kinematics, magnitude, and timing of deformation in the CNTB. We combine our findings with those of Di Fiori et al. (2020), a complementary study that described evidence for syn-contractional deposition within the type-exposure of the NCF in the southern Diamond Mountains. We then integrate our results with other published timing constraints for contractional deformation in the CNTB and surrounding regions of the Sevier hinterland, to place hinterland deformation in the larger space-time framework of deformation across the entire Cordilleran retroarc at this latitude.

## 2. Cordilleran Geologic Framework

During the late Neoproterozoic, western Utah and Nevada were located along the recently rifted western margin of the Laurentian craton (e.g., Dickinson, 2006). Deposition of Neoproterozoic to Lower Cambrian siliciclastic sedimentary rocks filled the accommodation generated by subsidence of the newly formed passive margin (e.g., Stewart & Poole, 1974). This was followed by shallow-marine deposition of a thick succession of carbonates between the Middle Cambrian and Devonian (e.g., Poole et al., 1992). During the Mississippian, passive margin sedimentation was interrupted by the Antler orogeny, which resulted in deep-water sedimentary rocks being thrust eastward over shallow-marine sedimentary rocks of the pe-

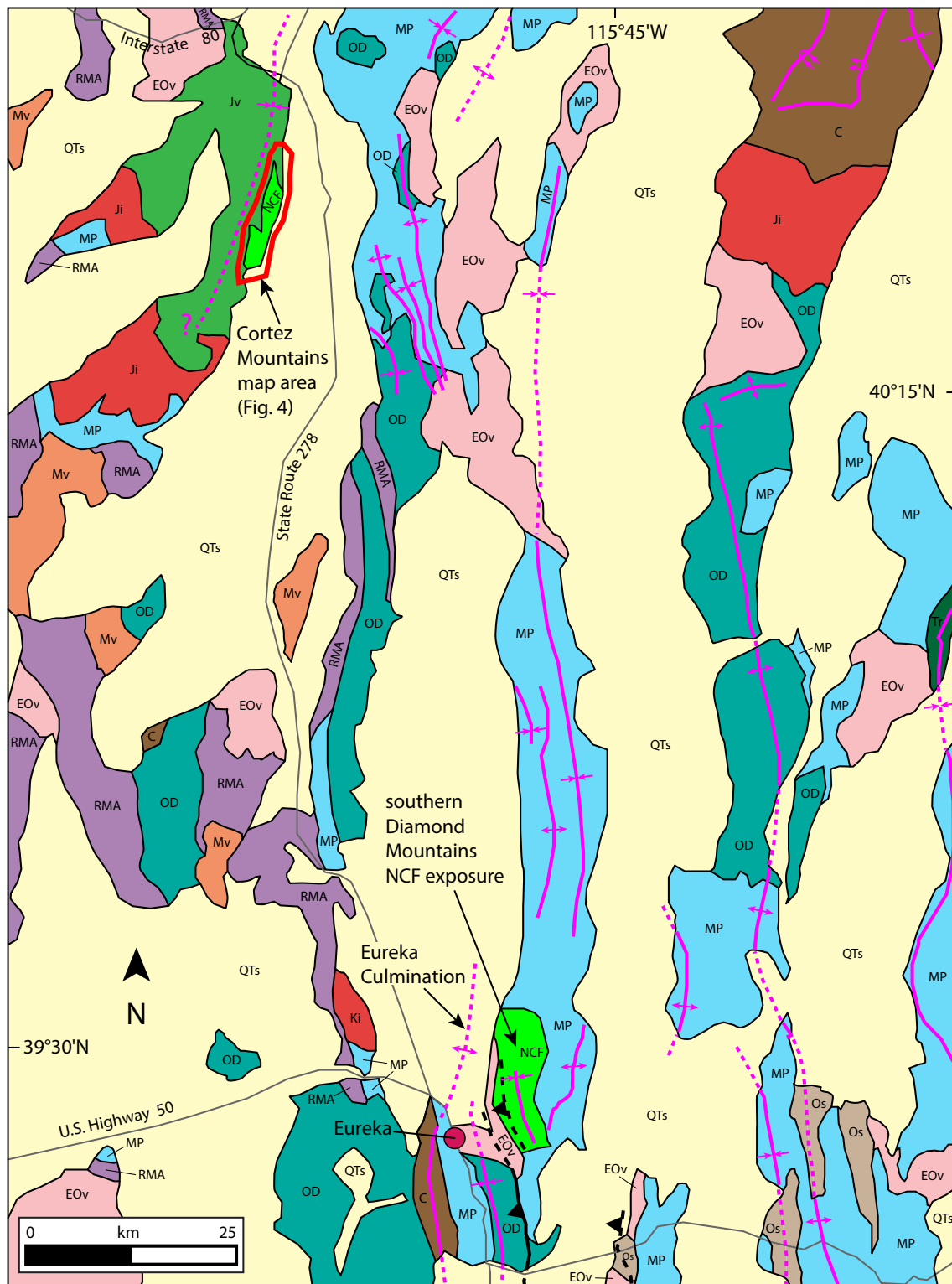


**Figure 2.** Geologic map of part of north-central Nevada. Geology was compiled and simplified from Crafford (2007) and Stewart and Carlson (1978), and the traces of Cordilleran folds and thrust faults are compiled from Colgan et al. (2010) and Long and Walker (2015). Exposures of the Newark Canyon Formation are shown in bright green and the Cortez Mountains map area from this study is outlined in red. See Figure 3 for a guide to map units.

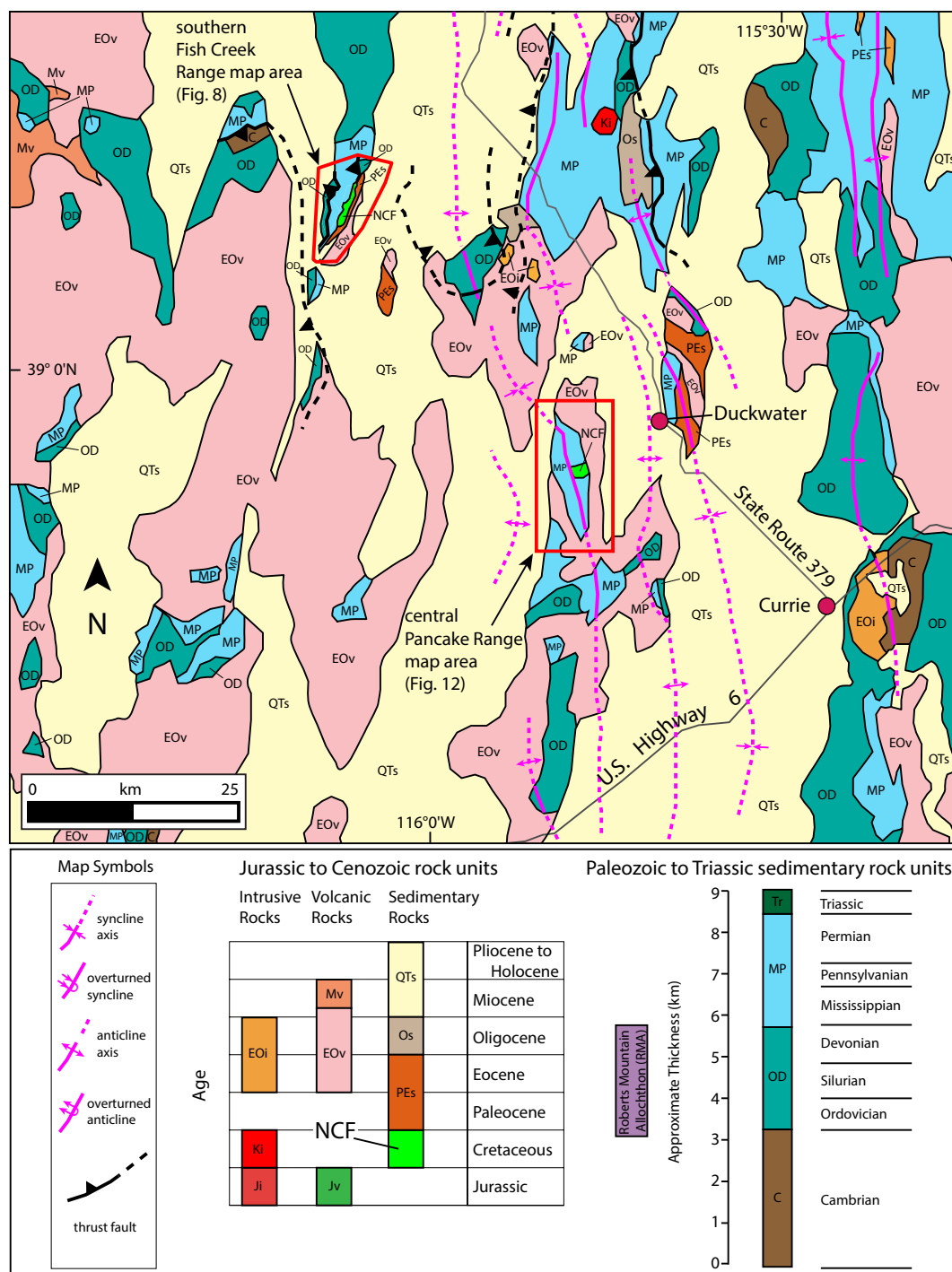


**Figure 3.** Geologic map of part of central Nevada, which is a southern continuation of Figure 2. Geology is compiled and simplified from Stewart and Carlson (1978) and Crafford (2007), and the traces of Cordilleran folds and thrust faults are compiled from Long and Walker (2015). Exposures of the Newark Canyon Formation are in shown in bright green and the southern Fish Creek Range and central Pancake Range map areas are outlined in red. The thickness scale for Cambrian-Triassic sedimentary rock units represents approximate average regional thicknesses from Stewart (1980), Smith and Ketner (1976), and Colgan et al. (2010).

ripheral continental shelf in central Nevada during west-directed subduction, and was likely the result of slab rollback (Burchfiel & Royden, 1991). This orogenic event generated subsidence of a foreland basin in eastern Nevada that was filled with clastic sediments that were eroded from the Antler highlands to the west (e.g., Dickinson, 2004, 2006; Poole et al., 1992). Following the Antler orogeny, shallow marine-dominated sedimentation continued in eastern Nevada through the Pennsylvanian-Triassic, with subsidence patterns interpreted to be controlled either by Ancestral Rockies tectonism to the east or the Sonoma orogeny to the west (e.g., Sturmer et al., 2018; Trexler et al., 2004).

During the Jurassic, the consolidation of the western margin of North America into an east-dipping, Andean-style subduction zone, initiated construction of the Cordilleran orogenic belt (e.g., Allmendinger, 1992; Burchfiel et al., 1992; DeCelles, 2004; Dickinson, 2004; Yonkee & Weil, 2015). Crustal shortening, magmatism, and metamorphism associated with Cordilleran orogenesis spanned from the Early Middle Jurassic to the Paleogene (e.g., DeCelles, 2004; Yonkee & Weil, 2015). The Cordillera, between the latitudes of  $\sim 36^{\circ}\text{N}$ – $\sim 42^{\circ}\text{N}$ , is divided into the Sierra Nevada magmatic arc in eastern California and a broad retroarc region that includes the Luning-Fencemaker thrust belt (LFTB) in western Nevada, the “Sevier hinterland” in central Nevada, eastern Nevada and westernmost Utah, and the Sevier fold-thrust belt in western Utah (Figure 1). The LFTB was constructed during the Middle-Late Jurassic closure of a back-arc basin (e.g., Oldow, 1984; Wyld, 2002). In the Sevier hinterland, Middle-Late Jurassic magmatism and associated contractional deformation have been documented in several areas of northeastern Nevada (e.g., Miller & Hoisch, 1995; Smith & Ketner, 1977; Zuza et al., 2020) and northwestern Utah (e.g., Allmendinger & Jordan, 1984).

Further to the south in Nevada and Utah, three structural provinces have been defined in the Sevier hinterland (Figure 1): The CNTB; the eastern Nevada fold belt; and the western Utah thrust belt. The CNTB branches off the Sevier fold-thrust belt in southern Nevada, and contains north-striking, east-vergent thrust faults and folds (Long, Henry, Muntean, Edmondo, & Cassel, 2014; Taylor et al., 2000). The Early Cretaceous NCF is exposed in several areas within and to the north of the CNTB. The eastern Nevada fold belt is a broad region to the east of the CNTB characterized by long wavelength, approximately north-trending folds (Long & Walker, 2015). The western Utah thrust belt accommodated  $\sim 10$  km of east-vergent shortening, and merges southward with the Sevier fold-thrust belt (Greene, 2014).

To the east in western Utah, the Sevier fold-thrust belt consists of a series of closely spaced, north-to-northeast-striking thrust faults and folds that accommodated  $\sim 150$ – $220$  km of shortening between the latest Jurassic and the Paleocene (e.g., DeCelles, 2004; DeCelles & Coogan, 2006; Yonkee & Weil, 2015; Yonkee et al., 2019). By the Late Cretaceous-Paleocene, eastern Nevada and westernmost Utah are interpreted to have been the site of an orogenic plateau (or “Nevadaplano”) with paleo-elevations up to  $\sim 2$ – $3$  km and crust up to  $\sim 45$ – $60$  km thick (e.g., Best et al., 2009; Cassel et al., 2014; Chapman et al., 2015; Colgan & Henry, 2009; Coney & Harms, 1984; DeCelles, 2004; Long, 2019; Snell et al., 2014; Vandervoort & Schmitt, 1990; Wells et al., 1990).

Following the termination of Cordilleran shortening, a northeast to southwest sweep of silicic volcanism across Nevada between the late Eocene and early Miocene, known as the “Great Basin ignimbrite flareup” (e.g., Best et al., 2009; Henry & John, 2013), has been attributed to rollback of the subducting Farallon plate (e.g., Humphreys, 1995; Smith et al., 2014). The ignimbrite flareup was broadly synchronous with early extension in several areas of eastern Nevada and western Utah (e.g., Druschke et al., 2011; Gans & Miller, 1983; Lee et al., 2017; Long, 2019; Long et al., 2018). During the Miocene, the western North American plate boundary underwent a significant reorganization, which resulted in the progressive termination of subduction of the Farallon plate and the concurrent growth of the San Andreas continental transform system (e.g., Atwater, 1970; Dickinson, 2002, 2006). From the Middle Miocene to the present, widespread normal faulting across Nevada and western Utah has constructed the Basin and Range Province, which is interpreted as a consequence of the demise of subduction and the change in relative plate motion vector that accompanied growth of the San Andreas transform system (e.g., Dickinson, 2002).

### 3. Previous Interpretations of the CNTB and NCF

Thrust faults and folds interpreted to be related to Cordilleran contractional deformation have been described in several early studies in central Nevada, particularly in the region surrounding the town of Eureka (Figures 1 and 2) (e.g., Nolan, 1962; Nolan et al., 1971, 1974). Later research grouped these thrust faults and folds together as the north-trending “Eureka thrust belt,” which spanned from  $\sim 38^{\circ}30'N$  to the northern border of Nevada (Heck et al., 1986; Speed, 1983; Speed et al., 1988), although minimal descriptions of the locations, geometry, style, and timing of structures were given. Following this, Taylor et al. (1993) and Taylor et al. (2000) described and correlated a series of east-vergent thrust systems in south-central Nevada between  $\sim 37^{\circ}N$  and the latitude of Eureka, and grouped them together genetically as the CNTB. Using cross section reconstructions, Taylor et al. (2000) estimated that the cumulative shortening accommodated in the CNTB was between  $\sim 10$  and  $\sim 15$  km. Most thrust faults in the southern part of the CNTB cut rocks as young as Pennsylvanian, and cross-cutting relationships with Late Cretaceous granite bodies indicate that motion on CNTB structures was completed by  $\sim 85$  Ma (Taylor et al., 2000). The CNTB is generally shown terminating northward at the latitude of Eureka, due to a lack of observations of surface-breaching thrust faults to the north (Figure 1). However, multiple north-trending fold axes have been mapped in the region to the north of the CNTB (Figure 2) (e.g., Colgan et al., 2010; Long & Walker, 2015).

In the northern part of the CNTB and proximal areas to the north, isolated exposures of the Early Cretaceous NCF (Figures 2 and 3), a terrestrial sedimentary unit postulated to have been deposited during regional thrust faulting and folding (e.g., Druschke et al., 2011; Fouch et al., 1979; Hose, 1983; Nolan et al., 1956; Vandervoort & Schmitt, 1990), offer the opportunity to further constrain CNTB deformation timing. Recent studies of the type-locality of the NCF in the southern Diamond Mountains (Figure 2) (Di Fiori et al., 2020; Long, Henry, Muntean, Edmondo, & Cassel, 2014) have documented that the NCF was deposited and deformed during construction of an east-vergent CNTB anticline named the Eureka culmination. Geologic mapping and U-Pb zircon geochronology showed that the NCF type-section exposure was deposited during growth of east-vergent folds and motion on associated thrust faults in the eastern limb of the culmination between  $\sim 114$  and  $< \sim 99$  Ma (Di Fiori et al., 2020).

Other NCF exposures in the surrounding region have the potential to offer important structural and temporal context for CNTB deformation. These exposures include the Cortez Mountains to the north of Eureka (Figure 2) and the southern Fish Creek Range and central Pancake Range to the south of Eureka (Figure 3). Fossils documented from the NCF in all three of these exposures have helped bracket their depositional age range. The NCF in the northern Cortez Mountains has yielded Cretaceous pollen, plant, and vertebrate fossils (e.g., Bonde et al., 2015; Smith & Ketner, 1976, 1978; Suydam, 1988). In the southern Fish Creek Range, the NCF has been interpreted as Early Cretaceous (Barremian to Albian) on the basis of invertebrate (Fouch et al., 1979) and vertebrate fossils (Bonde et al., 2015). The NCF in the central Pancake Range, which is the southernmost exposure known, has been interpreted as Upper Jurassic to Cretaceous based on a dinosaur fossil (Perry & Dixon, 1993). However, all three of these NCF exposures are lacking detailed structural context, as well as geochronology that can more precisely narrow down their depositional age. Below, we present geologic maps, stratigraphic divisions, and U-Pb zircon geochronology from each of these three NCF exposures.

## 4. Stratigraphy, Depositional Age, and Structural Geometry of the NCF in the Cortez Mountains Map Area

### 4.1. Lithostratigraphy

In the Cortez Mountains, the NCF is exposed in a 16-km-long, semi-continuous exposure on the eastern flank of the range (Figure 4). We have divided the NCF in the Cortez Mountains into five members (Kncc1–5; note: The additional “c” stands for “Cortez”, in order to differentiate from the members defined in the other two map areas), defined on the basis of dominant lithology and conglomerate clast composition (Figures 4 and 5; see the supporting information for photographs of representative outcrops). Kncc1 consists of weakly consolidated, clast supported, pebble to cobble conglomerate. Kncc2 is dominated by poorly indurated, massive mudstone with lenses of cross-stratified sandstone and conglomerate. Kncc3 consists of ridge-forming, red to brown, cross-stratified pebble to cobble conglomerate, which is interbedded with

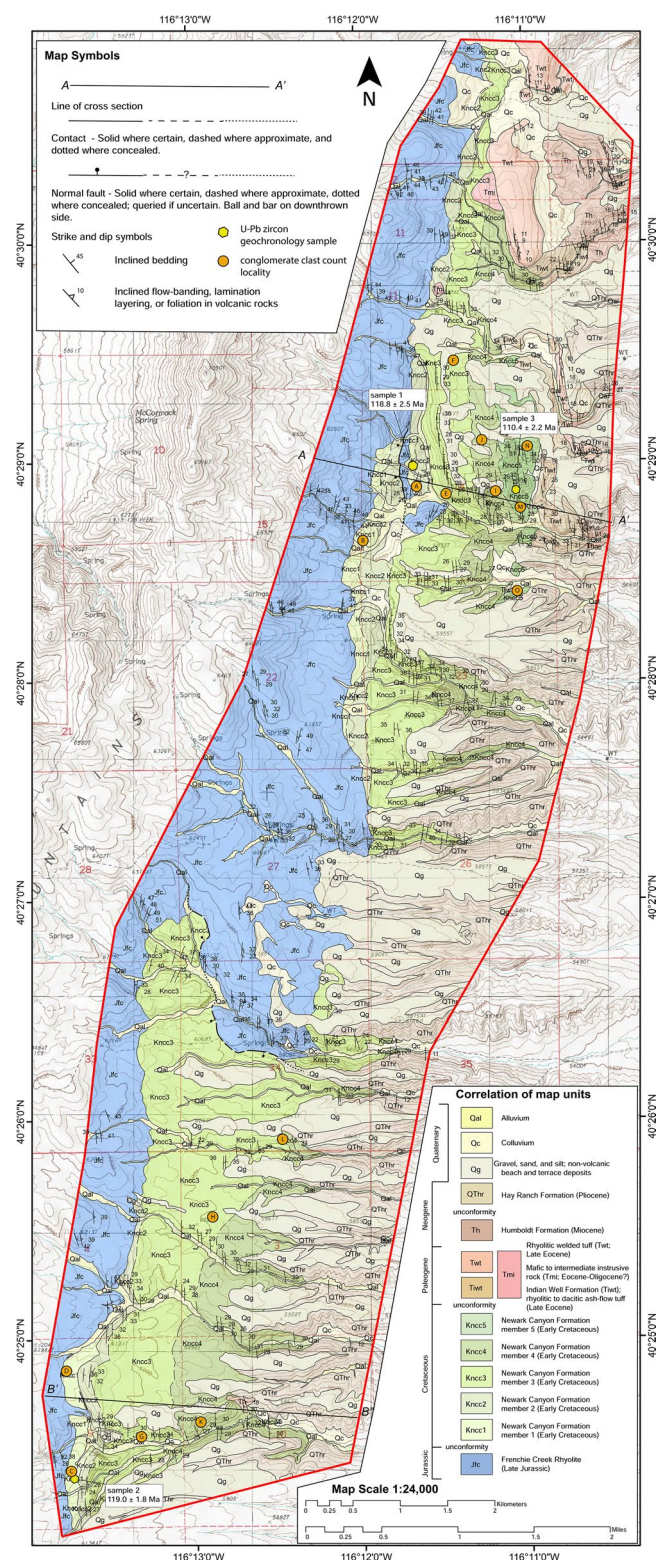


**Figure 4.** The 1:24,000-scale geologic map of the Newark Canyon Formation exposure (and proximal bedrock and surficial deposits) on the eastern flank of the northern Cortez Mountains.

massive and cross-bedded sandstone. Kncc4 is dominated by red-brown, massive and cross-stratified conglomerate and sandstone, which is interlayered with micrite and calcareous mudstone and siltstone. Kncc5 contains similar conglomerate and sandstone to Kncc4, but has a greater abundance of micrite, siliciclastic mudstone, siltstone, and pedogenic horizons. The NCF section in the Cortez Mountains has a cumulative thickness of 560 m (Figure 5).

In order to quantify the relative percentages of lithologies that comprise clasts within the NCF, clast composition counts were performed on conglomerate outcrops within NCF members (e.g., DeCelles, 1994; Dickinson, 1974, 1988; Horton et al., 2004). For each analysis, 100 clasts that were each  $\sim 3$  cm or larger in diameter were counted within a  $\sim 1$  m<sup>2</sup> area. Clast lithology categories included felsic volcanics, chert, carbonate, sandstone, quartzite, and pebble conglomerate. It is likely that less competent lithologies such as mudstone are under-represented in our clast counts. Clast count analyses were conducted at 15 different sites in the Cortez Mountains map area (Figure 4), with four analyses conducted each for members 1, 3, and 4, and three analyses conducted on member 5 (see supporting information for GPS locations and supporting data). The clast count data are shown in pie charts on Figure 5, with all clast count data from each NCF member combined into a single pie chart. Conglomerates in each NCF member contain between 26% and 41% chert. Kncc1 is dominated (60%) by felsic volcanic clasts that were likely sourced from erosion of the underlying Jurassic Frenchie Creek Rhyolite. Kncc3 exhibits an abundance (26%) of packstone carbonate clasts. Kncc4 and Kncc5 exhibit a larger percentage of sandstone (22%) and pebble conglomerate clasts (19%).

#### 4.2. Depositional Age Constraints

To constrain the depositional age range of the NCF in the Cortez Mountains map area, we performed U-Pb dating of zircon grains separated from three samples. Zircons were separated using a jaw crusher, disc-mill grinder, and water table, which was followed by magnetic and heavy liquid separation. The separated zircon grains were then mounted in epoxy resin, polished, and imaged via cathodoluminescence utilizing a microprobe at Washington State University (WSU). The zircons were analyzed using laser ablation inductively coupled plasma mass spectrometry at the WSU Radiogenic Isotope Laboratory (see supporting information for details on methods). Most zircons obtained from the NCF consisted of  $< 180$   $\mu\text{m}$  (*c*-axis) grains with varied degrees of roundness. Zircons that showed signs of damage (e.g., fractures or broken crystals) or that contained multiple inclusions were not analyzed. The  $^{206}\text{Pb}/^{238}\text{U}$  age was used as the “best age” for zircon grains that yielded ages younger than 900 Ma, while the  $^{207}\text{Pb}/^{206}\text{Pb}$  age was used for grains that yielded an age 900 Ma or older (e.g., Gehrels et al., 2008; Schoene, 2014). We defined cut-off discordance values for specific zircon grain age groups, including 15%–5% discordance for grains 900 Ma and older, 20%–10% discordance for grains that fell within the 900–300 Ma age range, and 25%–20% discordance for grains younger than 300 Ma (e.g., Chang et al., 2006; Gehrels et al., 2008). Using these discordance cut-offs, between 3% and 17% of the grains from individual samples were deemed unacceptable and were thus discarded. It is difficult to assess Pb-loss in zircon grains younger than 300 Ma (e.g., Bowring & Schmitz, 2003); however, we mitigate this

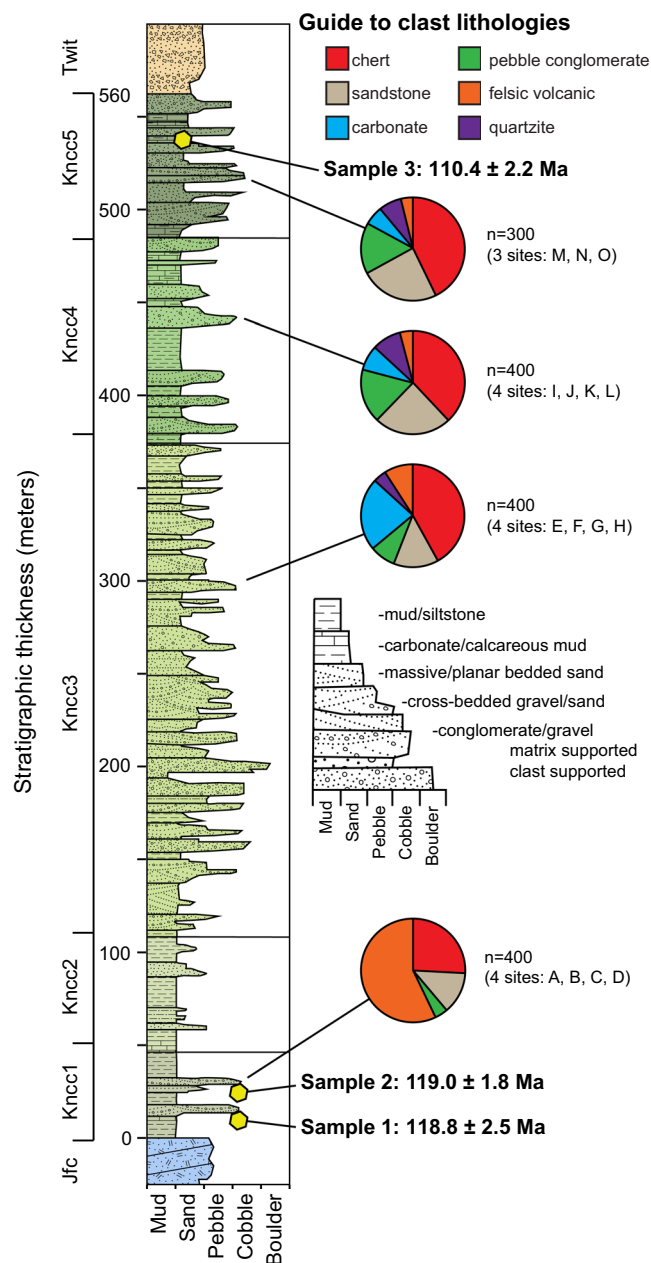


**Figure 5.** Stratigraphic column of the Newark Canyon Formation exposure in the northern Cortez Mountains (see Figure 4 for a guide to unit abbreviations). Pie charts of combined clast count data for each Newark Canyon Formation member are shown, as well as stratigraphic locations and ages of U-Pb zircon geochronology samples.

potential problem by implementing methods that rely on using multiple overlapping grain ages to define statistically significant age populations (Courtts et al., 2019; Dickinson & Gehrels, 2009).

Three NCF samples were collected from horizons interpreted to represent minimally reworked, waterlain tuffs in the Cortez Mountains map area (photographs of outcrops and GPS locations of samples can be found in the supporting information). The presence of glass shards and euhedral zircon grains in each sample supports this interpretation (see supporting information for photographs of zircon grains). Samples 1 and 2 were collected within member Kncc1 and sample 3 was collected within member Kncc5 (Figure 4). To obtain the youngest age group, euhedral zircon grains were picked and analyzed from samples 1–3. Twenty-nine euhedral zircons were analyzed from sample 1, and four of these grains were discarded for not meeting the discordance cut-off values. The youngest eight of the remaining 25 analyses define an age group that overlaps within error that yielded a weighted mean age (calculated using Isoplot; Ludwig, 2008) of  $118.8 \pm 2.5$  Ma ( $2\sigma$ ) (Figure 6). Thirty-seven zircons were analyzed from sample 2, with only a single discarded analysis. The 11 youngest overlapping zircons from sample 2 yielded a weighted mean age of  $119.0 \pm 1.8$  Ma ( $2\sigma$ ). Thirty-eight zircons were analyzed from sample 3, and the youngest twenty-four grains that overlap within error yield a weighted mean age of  $110.4 \pm 2.2$  Ma ( $2\sigma$ ).

All three tuff samples are interpreted to have been minimally reworked at the time of deposition, and we interpret the Concordia ages of the youngest group of overlapping zircon grains as actual ages of deposition due to the lack of evidence for significant detrital mixing. Therefore, NCF deposition in the Cortez Mountains map area can be bracketed between  $\sim 123$  and  $117$  Ma (Aptian), the timing of deposition of Kncc1, and  $\sim 110$ – $108$  Ma (Albian), the timing of deposition of Kncc5. These depositional ages are compatible with published timing estimates from fossil assemblages. Reptile and ankylosaur teeth and bones sampled from near the base the NCF exposure (our member Kncc1) have been determined to be from the Jurassic or Cretaceous, and fossil flora and pollen data suggest a Cretaceous deposition age (Smith & Ketner, 1976). Dinosaur bones collected and described by Bonde et al. (2015) are also compatible with an Early Cretaceous deposition age.

Samples 1–3 all yielded an older population of zircons between  $\sim 140$  and  $\sim 165$  Ma (Figure 6), which we interpret as the result of incorporation of inherited zircons during minor, syn-depositional reworking. We interpret that the most likely origin for these older zircons is from erosion of the underlying Late Jurassic Frenchie Creek Rhyolite. It is also possible that older zircon grains were incorporated during ash eruption, or that inherited zircon cores were dated.

### 4.3. Structural Geometry

In most places in the Cortez Mountains map area, the NCF disconformably overlies the Upper Jurassic Frenchie Creek Rhyolite (Figures 4 and 7), although a gentle ( $<10^\circ$  of dip difference) angular unconformity between the two units was locally observed. The Frenchie Creek Rhyolite and the overlying NCF both are north-striking and exhibit a homogenous dip of  $\sim 25$ – $35^\circ$ E. The NCF section lacks any record of intraformational, syn-depositional folding, faulting, or unconformities. The NCF is disconformably overlain by late Eocene rhyolitic ash-flow tuffs, which exhibit a similar  $\sim 25$ – $35^\circ$  average eastward dip. Above these

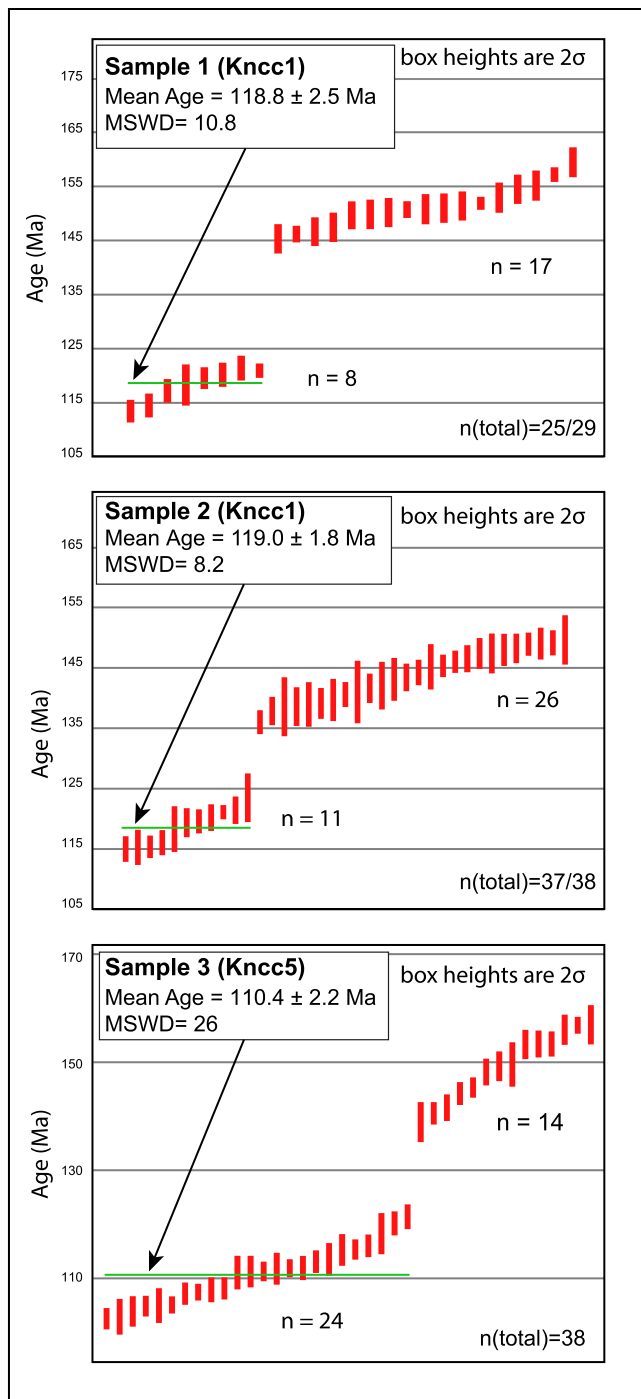


**Figure 6.** Weighted mean plots for samples of waterlain tuff collected from the basal (Kncc1; samples 1 and 2) and highest (Kncc5; sample 3) members of the Newark Canyon Formation in the northern Cortez Mountains (generated in Isoplot; Ludwig, 2008). The youngest group of overlapping ages were used to determine an average age for each sample. Error bar heights are shown at  $2\sigma$ . mean square of weighted deviates values presented here were calculated for the youngest age population of concordant grains.

tuffs, middle Miocene sedimentary rocks of the Humboldt Formation dip slightly shallower ( $\sim 15^{\circ}$ – $20^{\circ}$ ) to the east, defining a gentle angular unconformity at the top of the late Eocene tuffs.

#### 4.4. Tectonostratigraphic Interpretation

The NCF exposure in the Cortez Mountains map area does not exhibit any evidence for syn-depositional or post-depositional contractional deformation. However, on the western side of the Cortez Mountains, directly west of the southern part of our map area, Late Jurassic volcanic and volcanoclastic rocks exhibit intraformational angular unconformities (Muffler, 1964) (Figures 7a and 7c), which we here interpret to bracket the timing of regional folding. The oldest Late Jurassic unit, the Big Pole Formation, dips steeply ( $\sim 30^{\circ}$ – $80^{\circ}$ ) northwest, and is overlain by the moderately ( $\sim 25^{\circ}$ – $45^{\circ}$ ) east-dipping Late Jurassic Sod House Tuff and  $151 \pm 3$  Ma (K-Ar biotite; Smith & Ketner, 1976) Frenchie Creek Rhyolite (Muffler, 1964). This defines an angular unconformity that records significant Late Jurassic tilting after deposition of the Big Pole Formation but prior to the deposition of the Sod House Tuff. Additionally, the disconformity observed between the Frenchie Creek Rhyolite and the NCF indicates a lack of significant tilting or folding after  $\sim 151$  Ma. This is consistent with mapped relationships of undeformed, shallowly emplaced alaskite intrusions in the western part of the range (Figure 7a), which intrude all three Late Jurassic volcanic and volcanoclastic units, and have yielded K-Ar hornblende ages of  $150 \pm 23$  Ma,  $145 \pm 22$  Ma, and  $125 \pm 19$  Ma (Muffler, 1964).

We speculate that the differential tilting exhibited between Late Jurassic volcanic units in the Cortez Mountains is related to regional Mesozoic folding. After retro-deformation of the eastward tilting of the Frenchie Creek Rhyolite, the Big Pole Formation to the west of our map area restores to an approximate orientation of  $033^{\circ}$ ,  $86^{\circ}$ NW (see supporting information for a supporting stereonet), and therefore, may represent a portion of the limb of an anticline or syncline. We interpret that Late Jurassic folding in the Cortez Mountains could be related temporally to northeast-trending folds mapped in the Adobe Range  $\sim 40$  km to the northeast, which deform rocks as young as Triassic (Ketner & Alpa, 1992; Smith & Ketner, 1977).

The disconformity between the NCF and the underlying Frenchie Creek Rhyolite, combined with the lack of evidence for syn-depositional or post-depositional thrust faulting or folding of the NCF, indicate that contractional deformation in the Cortez Mountains map area was complete prior to NCF deposition. Additionally, the disconformity between the NCF and overlying late Eocene volcanic rocks (Figures 4 and 7) indicates that the  $\sim 25^{\circ}$ – $35^{\circ}$  of eastward tilting exhibited by both units was accommodated after the late Eocene. We interpret that this tilting is the result of regional Basin and Range normal faulting (e.g., Colgan et al., 2010; Colgan & Henry, 2009). The shallower ( $\sim 15^{\circ}$ – $20^{\circ}$ ) eastward dip of the overlying middle Miocene Humboldt Formation (Figures 4 and 7) indicates that normal fault-related tilting must have begun prior to its deposition.

We interpret that clast composition data from the NCF define the progressive unroofing of deeper stratigraphic levels within a proximal source region. The abundant felsic volcanic clasts in member Kncc1 (Figure 5)

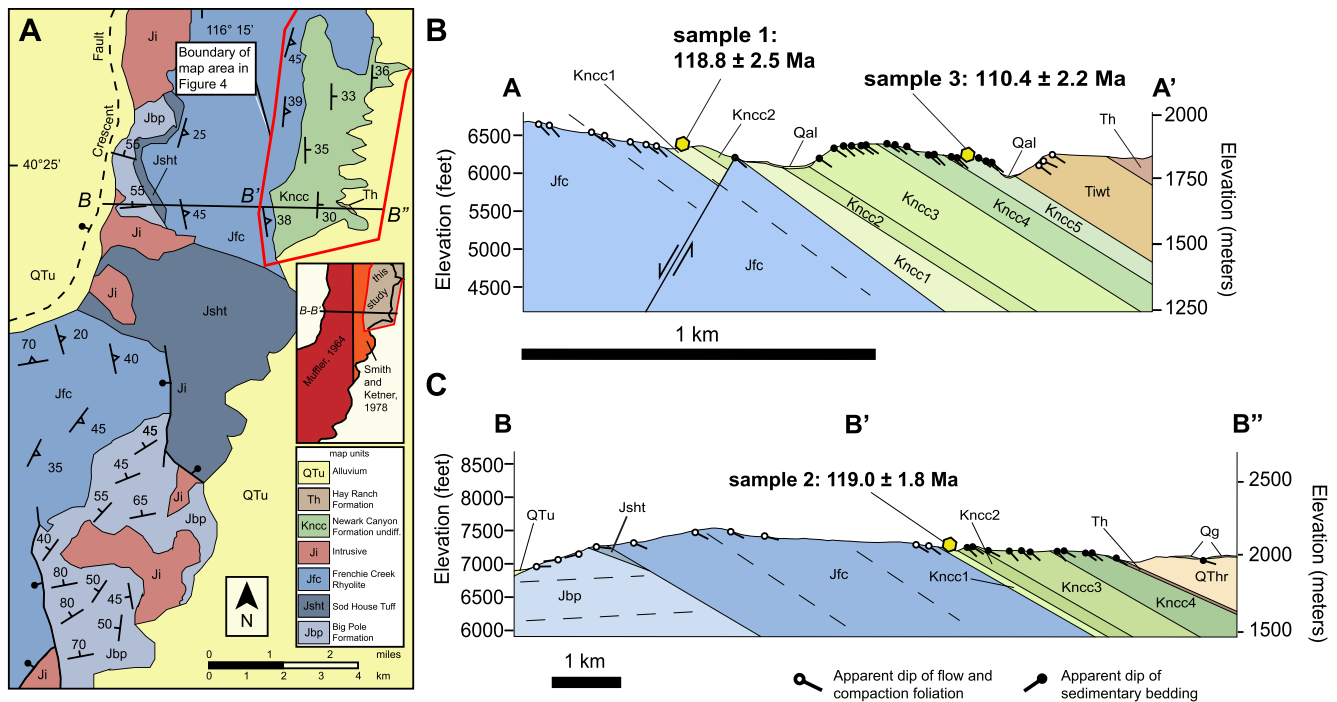


**Figure 7.** (a) Simplified geologic map of the central part of the Cortez Mountains (compiled from Muffler, 1964; Smith & Ketner, 1978, and this study), which highlights angular unconformities within volcanics of the Late Jurassic Pony Trail Group (units Jbp, Jsht, and Jfc) to the west of our map area. (b) Cross section A-A' through the northern portion of the Cortez Mountains map area (line of section and guide to map units shown on Figure 4). (c) Cross section B-B' through the southern portion of the Cortez Mountains map area and adjacent area to the west (line of section and guide to map units shown on Figures 4 and 7a), which highlights angular unconformities between units of the Late Jurassic Pony Trail Group (units Jbp, Jsht, and Jfc).

likely indicate erosion of proximal Late Jurassic volcanic rocks, which immediately underlie the basal NCF unconformity. The age groups of Jurassic grains obtained from samples 1 and 2 (Figure 6) overlap with the  $151 \pm 3$  Ma age for the underlying Frenchie Creek Rhyolite from Smith and Ketner (1976), which indicates that the volcanic clasts within unit Kncc1 were likely sourced from erosion of the Frenchie Creek Rhyolite. Upsection, Kncc3 exhibits an abundance of carbonate clasts (Figure 5), which we interpret to be sourced from proximal Pennsylvanian-Permian carbonate units to the west of the map area (Figure 2; Muffler, 1964). Members Kncc4 and Kncc5 exhibit higher percentages of sandstone and pebble conglomerate clasts (Figure 5), which we speculate may have been sourced from rocks as young as Permian, which regionally contain carbonates interlayered with sandstone and conglomerate (e.g., Stewart, 1980), or as old as the Mississippian Antler foreland basin clastic section (e.g., Di Fiori et al., 2020).

Using trough cross-bedding axis orientations and pebble imbrication orientations, Suydam (1988) measured an average paleocurrent vector of east-southeast for the NCF in the Cortez Mountains map area. Combining this paleocurrent data with the unroofing sequence defined in our clast composition data, we interpret that the NCF was sourced from erosion of proximal Jurassic and Mississippian-Permian rocks that lay to the west-northwest. Though structural evidence for syn-NCF contractional deformation is lacking in our map area, we speculate that the most likely scenario for triggering erosion and generating the accommodation for NCF deposition is an Early Cretaceous (~119–110 Ma) thrusting and/or folding event to the west. This deformation likely generated a topographic high that was progressively eroded from Jurassic to Upper Paleozoic stratigraphic levels, which shed clastic sediments of the NCF eastward. This scenario, though speculative, is compatible with syn-contractional deposition of the NCF between ~115 and ~100 Ma that is documented ~100 km to southeast in the southern Diamond Mountains (Figure 2; Di Fiori et al., 2020).

## 5. Stratigraphy, Depositional Age, and Structural Geometry of the NCF in the Southern Fish Creek Range Map Area

### 5.1. Lithostratigraphy

In the southern Fish Creek Range map area, the NCF is exposed in a ~14-km-long continuous exposure on the eastern flank of the range (Figure 8). We have divided the NCF in this map area into four members, which have a cumulative thickness of 325 m (Figures 8 and 9; a photograph of a representative outcrop is shown in the supporting information). The basal member (Kncf1, with the “f” denoting NCF from the Fish Creek Range) consists of cross-stratified, clast-supported, pebble conglomerate, interbedded with cross-bedded, normally graded, medium-to-coarse-grained sandstone. Kncf2 is characterized by medium-grained, well-bedded, horizontally to trough cross-bedded sandstone with lenses of clast-supported pebble conglomerate. Kncf3 consists of weakly indurated calcareous mudstone and siltstone. The highest member (Kncf4) is characterized by white to cream colored, massive, well-bedded micrite interstratified with mudstone and siltstone.

Conglomerate clast composition counts were performed on members Kncf1 and Kncf2, using the same methods described above in Section 4.1 (supporting data in the supporting information) (Figure 9). Two clast count analyses were conducted on Kncf1, which yielded an abundance (55%) of chert and a significant population (25%) of carbonate clasts. Two analyses were conducted on Kncf2, which also yielded abundant (63%) chert clasts, but significantly less (11%) fine-crystalline carbonate clasts. Both members yielded similar percentages of quartzite and sandstone clasts (8%–13% and 12%, respectively).

In the Fish Creek Range, the Sheep Pass Formation unconformably overlies the NCF, and consists of red-to-orange-weathering, massive, clast supported conglomerate. This unit has previously been interpreted to have a Maastrichtian-Paleocene depositional age range based on lithologic similarities with Sheep Pass Formation exposures in nearby mountain ranges in eastern Nevada (Druschke et al., 2011; Fouch et al., 1979; Hose, 1983); however, no fossils from the Sheep Pass Formation in the southern Fish Creek Range have yet been described. The thickness of the Sheep Pass Formation in our map area is ~50 meters (Figure 9).

### 5.2. Depositional Age Constraints

We performed U-Pb dating of zircons separated from two samples collected in the southern Fish Creek Range map area, using the same methods as described above in Section 4.2. We did not observe any tuffs, so we collected two samples (samples 4 and 5) for dating of detrital zircons (Figure 10). For these detrital samples, we calculated maximum depositional ages (MDA) utilizing the “youngest 1 $\sigma$  grain cluster” (or “YC1 $\sigma$ (2+)”) method outlined in Dickinson and Gehrels (2009), which was recently evaluated by Coutts et al. (2019). This method uses the weighted mean age of the five youngest zircon grains that overlap within error to estimate a conservative MDA.

Sample 4 was collected from a medium-grained sandstone in the middle portion of Kncf1 (Figures 8 and 9). A total of 160 grains were analyzed, with 149 of these passing the discordance cut-off requirements. This sample yielded a youngest prominent peak at ~155 Ma ( $n = 8$ ), with older, less prominent peaks at ~360, ~560, and ~1,050 Ma (Figure 10). The five youngest grains that overlapped within error yielded an MDA of  $130.6 \pm 2.6$  Ma ( $2\sigma$ ).

The NCF in the southern Fish Creek Range has been previously interpreted to have been deposited during the Early Cretaceous (Berremian-Albian) based on assemblages of ostracods, charophytes, and palynomorphs (Fouch et al., 1979). Later work by Bonde et al. (2015) documented vertebrate fossils from rocks that we map as member Kncf3, which were interpreted to be Aptian or younger. Our U-Pb detrital zircon geochronology is in agreement with these depositional timing estimates. Our MDA of  $130.6 \pm 2.6$  Ma from basal member Kncf1 indicates that the NCF in the southern Fish Creek Range was deposited no earlier than the Hauterivian stage of the Early Cretaceous. Combining our geochronologic data with published fossil assemblage interpretations, deposition of the NCF in the southern Fish Creek Range map area can be bracketed between the Hauterivian (~133 Ma) and Albian (~100 Ma) (Bonde et al., 2015; Fouch et al., 1979; this study).

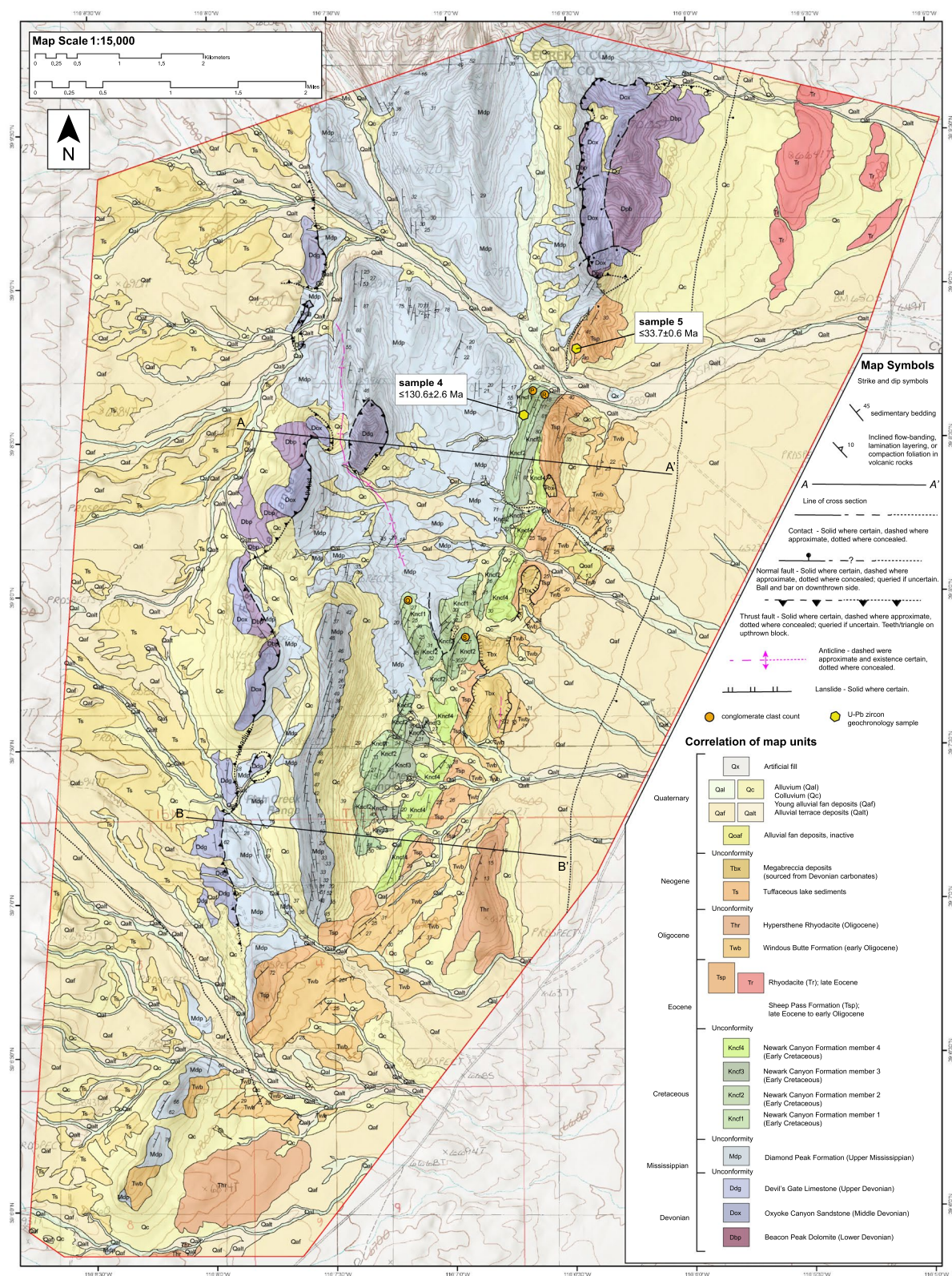
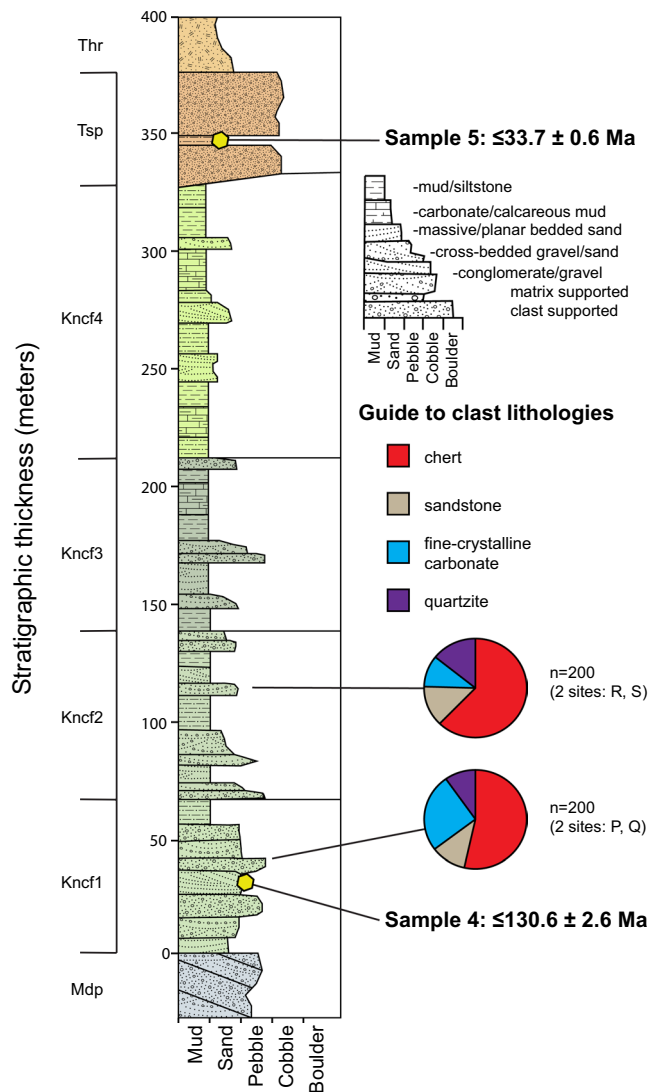


Figure 8. The 1:15,000-scale geologic map of the southern Fish Creek Range.



**Figure 9.** Stratigraphic column of the Newark Canyon Formation and Sheep Pass Formation in the southern Fish Creek Range (see Figure 8 for a guide to unit abbreviations). Pie charts of combined clast count data for two Newark Canyon Formation members are shown, as well as stratigraphic locations and maximum depositional ages of U-Pb zircon geochronology samples.

Sample 5 was collected from a sandstone horizon near the base of the Sheep Pass Formation (unit Tsp), which overlies the NCF (Figures 8 and 9). A total of 163 grains were analyzed, with 144 meeting the discordance cutoff requirements. Sample 5 yielded a youngest peak ( $n = 7$ ) centered at  $\sim 33$  Ma, and older peaks at  $\sim 1,830$  and  $\sim 2,695$  Ma (Figure 10). The five youngest grains that overlapped within error yielded an MDA of  $33.7 \pm 0.6$  Ma.

The Sheep Pass Formation in the southern Fish Creek Range has been previously interpreted as Maastrichtian to Paleocene in age on the basis of lithologic comparison to similar conglomerate in the Egan Range (Fouch et al., 1979; Hose, 1983; Kellogg, 1964). However, the  $33.7 \pm 0.6$  Ma MDA that we obtained from sample 5 indicates that this unit was deposited no earlier than the latest Eocene in the Fish Creek Range. Additionally, the Sheep Pass Formation is overlain by the Windous Butte Formation, a rhyolitic tuff that has been dated at  $32.5 \pm 0.8$  to  $32.3 \pm 1.0$  Ma (K-Ar sanidine; Hose, 1983). This allows bracketing the timing of Sheep Pass Formation deposition between 34.2 and 31.3 Ma (Late Eocene to Early Oligocene).

### 5.3. Structural Geometry

There are north-striking contractional structures exposed in the southern Fish Creek Range, including several isolated exposures of shallowly ( $\sim 10$ – $25^\circ$ ) west-dipping, east-vergent thrust faults that place Devonian carbonates over Mississippian clastic rocks (Figures 8 and 11). We interpret that these isolated exposures of Devonian rocks represent erosional remnants of the hanging wall of what once was a continuous, through-going thrust fault, which we name the Vanadium thrust after nearby historical vanadium prospects. The Vanadium thrust cuts rocks as young as Mississippian within its footwall, which typically dip moderately to the east. However, within the north-central part of the map area, these Mississippian rocks have been folded into a north-northwest-trending anticline (Figures 8 and 11). A minimum offset magnitude for the Vanadium thrust can be estimated from the east-west outcrop extent of Devonian hanging wall rock units in the northern part of the map area, which define a minimum east-west structural overlap of  $\sim 4.2$  km (Figure 8). No cross-cutting relationships between the Vanadium thrust and the NCF or the Sheep Pass Formation are exposed (Figure 8).

The NCF overlies Mississippian sedimentary rocks across an angular unconformity with up to  $\sim 20^\circ$  of difference in dip (Figures 8 and 11).

The NCF typically exhibits a moderate dip of  $\sim 30^\circ$ E, but locally dips as steeply as  $\sim 70^\circ$ E– $80^\circ$ E (Figures 8 and 11). The unconformity between the NCF and the overlying Sheep Pass Formation is a disconformity in several parts of the map area, but locally exhibits as much as  $\sim 20^\circ$ – $50^\circ$  of difference in dip angle (Figures 8 and 11). The Sheep Pass Formation and overlying Oligocene volcanic units exhibit a homogeneous dip of  $\sim 25^\circ$ E– $30^\circ$ E.

### 5.4. Tectonostratigraphic Interpretation

Motion on the Vanadium thrust can be bracketed as Late Mississippian or younger, but the lack of exposed cross-cutting relationships between the Vanadium thrust and the NCF does not allow narrowing the timing of motion any further. However, we interpret that it is likely that the Vanadium thrust is genetically related to Cordilleran (i.e., Late Mesozoic) shortening accommodated regionally within the CNTB. This interpretation is supported by observations of multiple north-striking, east-vergent thrust faults and folds along-strike

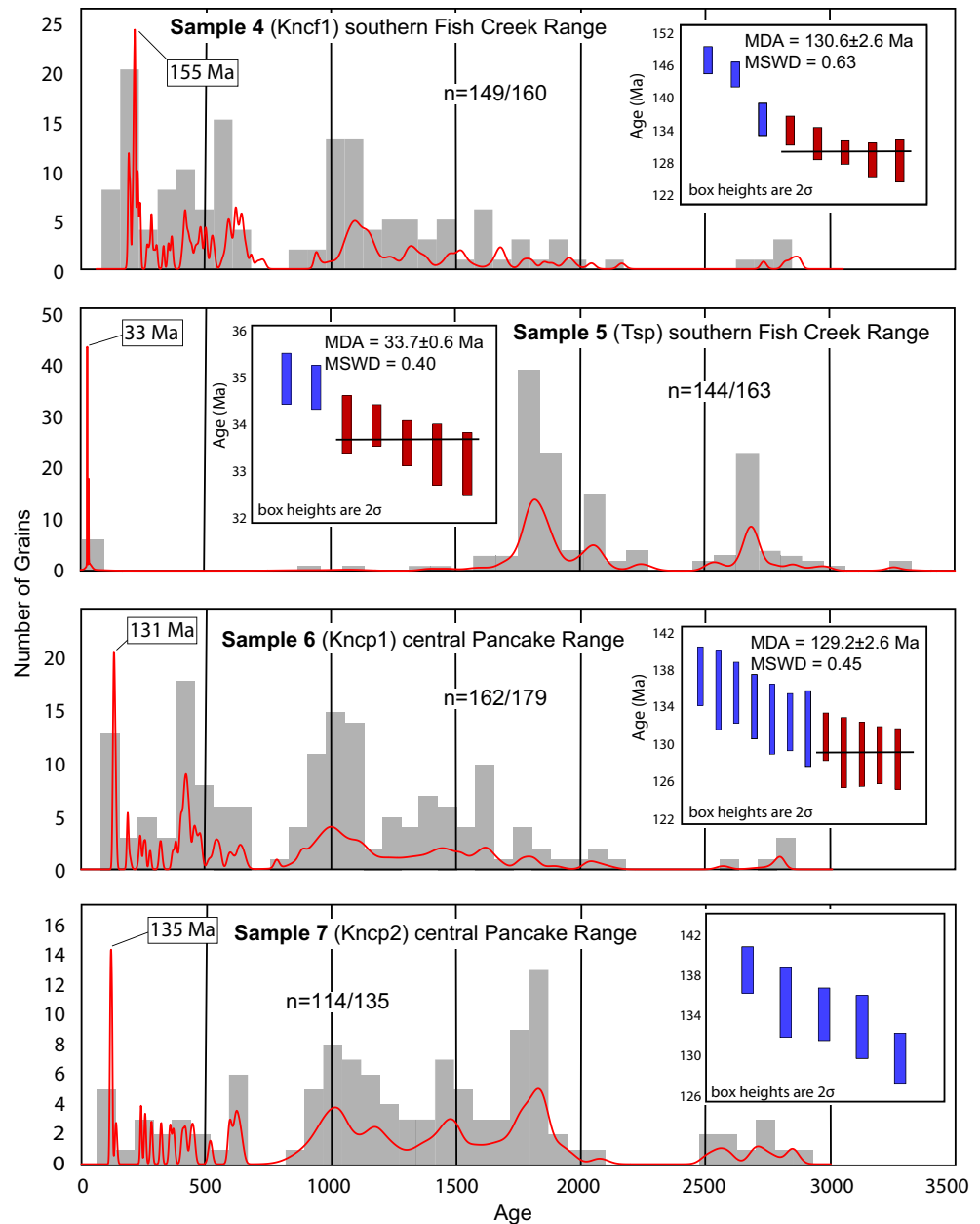


**Figure 10.** Probability density plots for U-Pb detrital zircon analyses of Newark Canyon Formation and Sheep Pass Formation samples from the southern Fish Creek Range (samples 4 and 5) and central Pancake Range (samples 6 and 7). The center ages of major Mesozoic and Cenozoic peaks are labeled (determined in Isoplot; Ludwig, 2008). The number of grains plotted (based on concordance criteria defined in the text) out of total grains analyzed (e.g.,  $n = 99/127$ ) is shown for each sample. Inset graphs show all grain ages that define the youngest age peak for each sample (generated using the zircon age extraction tool in Isoplot; Ludwig, 2008). The weighted mean age of the five youngest grains that overlap within error (the  $YC1\sigma(2+)$  method of Dickinson & Gehrels, 2009; grains utilized in the calculation are highlighted in red) is interpreted as the MDA for each sample, and is shown with a black line. Errors on MDA's are reported at the  $2\sigma$  level. No MDA was calculated for sample 7 because it did not yield five Mesozoic zircon grains that overlapped within error. However, sample 7 did yield five grains between  $\sim 140$  and  $\sim 130$  Ma, which are plotted on the inset graph. MSWD, mean square of weighted deviates.

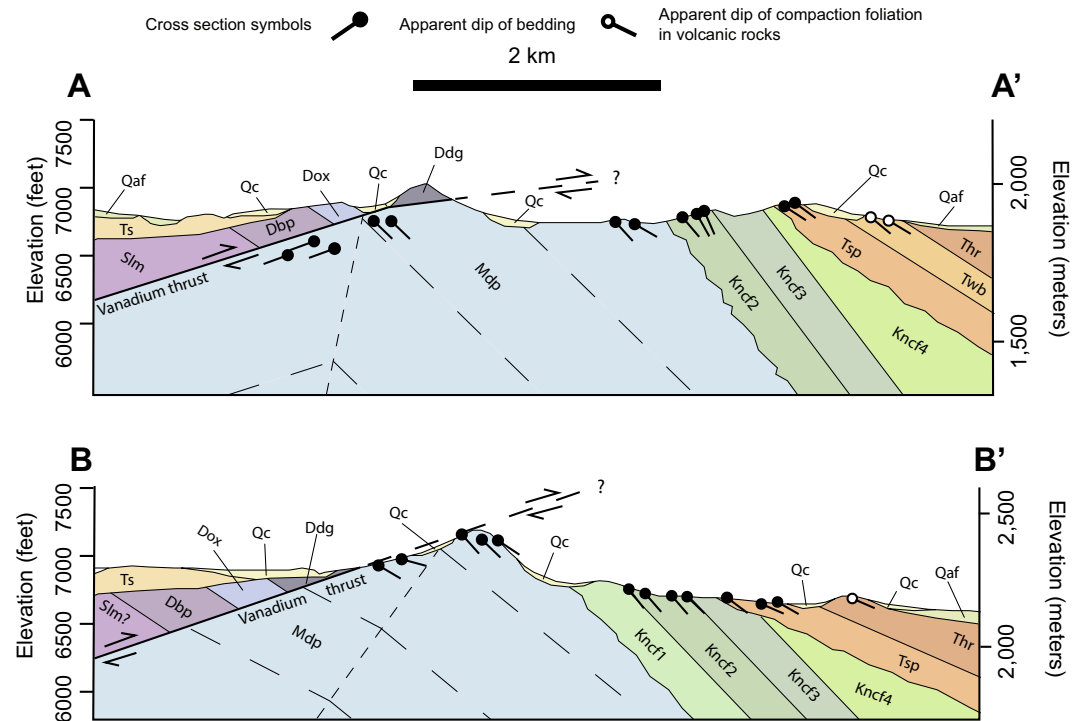


**Figure 11.** Cross sections A-A' and B-B' through the southern Fish Creek Range map area. See Figure 8 for section line locations and a guide to unit abbreviations.

to the north in the Fish Creek Range and Diamond Mountains and to the east in the Pancake Range, all of which have been interpreted as components of the CNTB (Figure 3) (e.g., Carpenter et al., 1993; Di Fiori et al., 2020; Hose, 1983; Long, 2012; Long, Henry, Muntean, Edmondo, & Cassel, 2014; Long & Walker, 2015; McDonald, 1989; Nolan et al., 1974; Taylor et al., 1993; Taylor et al., 2000).

Three additional lines of evidence potentially allow linking deposition of the NCF temporally with motion on the Vanadium thrust. First, Vandervoort (1987) measured paleocurrent directions in the NCF from imbricated pebble clasts and cross-bedding orientations, which define a dominant east-southeast sediment transport direction ( $\sim 106^\circ$  average azimuth), indicating that the source area for the NCF was from the west-northwest. Second, conglomerates in Kncl1 and Kncl2 both exhibit populations ( $\sim 10\%$ – $30\%$ ) of crystalline dolostone clasts, which were most likely sourced from proximal Devonian carbonate units carried in the hanging wall of the Vanadium thrust. This indicates that the Devonian source rocks had to have been exposed at the surface at the time of NCF deposition; although this does not preclude motion on the Vanadium thrust pre-dating NCF deposition, this does support the interpretation that motion on the thrust does not post-date NCF deposition. Third,  $\sim 35$  km to the north, in the southern Diamond Mountains, Di Fiori et al. (2020) documented field relationships between the Lower Cretaceous ( $\sim 115$ – $100$  Ma) NCF and thrust faults and folds of the CNTB that define syn-contractual NCF deposition, and indicate that CNTB structures were responsible for generating the accommodation in which the NCF accumulated (Fetrow et al., 2020).

In summary, although the southern Fish Creek Range map area lacks field relationships that definitively relate Lower Cretaceous NCF deposition to motion on the Vanadium thrust, we interpret that it is likely that this thrust fault generated a topographic high to the west from which source material for the NCF was derived, and produced accommodation to the east within its footwall, in which the NCF was deposited. This interpretation is supported by paleocurrent directions, clast compositions, and comparison to proximal NCF exposures.

Following its deposition, the angular unconformity between the NCF and the Sheep Pass Formation indicates that the NCF was locally tilted as much as  $\sim 20^\circ$ – $50^\circ$  eastward prior to the late Eocene. This could have

been the result of growth of a separate CNTB fold, perhaps a syncline that has its axis concealed beneath Quaternary overburden in Little Smokey Valley to the east. We consider this to be a plausible scenario based on geologic mapping to the east in the Pancake Range (e.g., Kleinhampel & Ziony, 1985; McDonald, 1989; Perry & Dixon, 1993) and to the north in the Fish Creek Range and Diamond Mountains (e.g., Di Fiori et al., 2020; Long, 2012; Long, Henry, Muntean, Edmondo, & Cassel, 2014; Long, Henry, Muntean, Edmondo, & Thomas, 2014; Long & Walker, 2015; Nolan et al., 1974, 1971), that has identified multiple north-trending CNTB folds.

Above the NCF, the late Eocene-early Oligocene Sheep Pass Formation and overlying Oligocene volcanic units exhibit a uniform 25°–30° eastward dip. We attribute this moderate dip to Neogene east-west extension and related rotation during regional Basin and Range normal faulting (Stewart, 1980).

## 6. Stratigraphy, Depositional Age, and Structural Geometry of the NCF in the Central Pancake Range Map Area

### 6.1. Lithostratigraphy

In the central Pancake Range map area, the NCF is only preserved in a single isolated exposure near the center of the map (Figure 12). Here, we mapped the NCF as a single, 30-m-thick unit (Kncp; the “p” denotes the Pancake Range) and did not divide it into members (Figure 13a). The basal ~14 m of the NCF are dominated by weakly indurated, dark gray mudstone with interbeds of siltstone and fine-grained sandstone. Above the mudstone is ~7 m of ledge-forming, gray, clast-supported, pebble-to-cobble conglomerate. Above this is ~9 m of yellow to brown micrite interbedded with medium-to-coarse-grained sandstone with abundant stromatolites.

Two clast count analyses were performed on the conglomerate in the middle of the section (Figure 13a), using the same methods discussed above in Section 4.1. The data define a dominance (85%) of coarse-crystalline carbonate clasts.

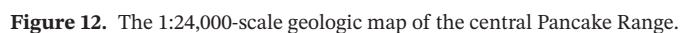
### 6.2. Depositional Age Constraints

Using similar methods as described above in Sections 4.2 and 5.2, we performed U-Pb dating of detrital zircons from two NCF samples (samples 6 and 7) collected from the central Pancake Range map area (Figures 12 and 13). Sample 6 was collected from an outcrop of sandy mudstone near the base of the NCF section. A total of 179 detrital zircon grains were analyzed from sample 6, with 162 of these passing the discordance cut-off requirements. Zircons from sample 6 yielded peaks centered at ~130, ~420, and ~1,010 Ma (Figure 10). The five youngest overlapping grains from sample 6 yielded an MDA of  $129.2 \pm 2.6$  Ma ( $2\sigma$ ). Sample 7 was collected from the matrix of the ledge-forming conglomerate in the middle of the NCF section. A total of 135 grains were analyzed from sample 7, with 114 meeting the discordance cut-off requirements. Sample 7 yielded peaks at ~140, ~630, ~1,040, ~1,470, and ~1,850 Ma. We did not calculate an MDA for sample 7 because the youngest grain group didn’t meet the five-overlapping-grain criterion that we defined above. However, there were four youngest grains from this sample that overlapped within error between ~130 and ~139 Ma (Figure 10), and a statistically significant youngest peak on the probability density plot at ~135 Ma, which likely indicates a similar (if slightly older) youngest grain population to sample 6.

The ~129 Ma MDA from sample 6 at the base of the NCF indicates that deposition occurred no earlier than the Barremian stage of the Early Cretaceous. This depositional age constraint is compatible with dinosaur bones that have been collected from the NCF basal mudstone, which indicate a Cretaceous depositional age (Perry & Dixon, 1993). These constraints collectively narrow NCF deposition between the Barremian stage and the end of the Cretaceous (~129–66 Ma).

### 6.3. Structural Geometry

The map-scale structural geometry of the central Pancake Range is dominated by the McClure Spring syncline, a north-northwest-trending syncline with an overturned (~40°W average dip) western limb and an upright eastern limb that dips an average of ~45° to the west-southwest (Figures 12 and 13). By comparing



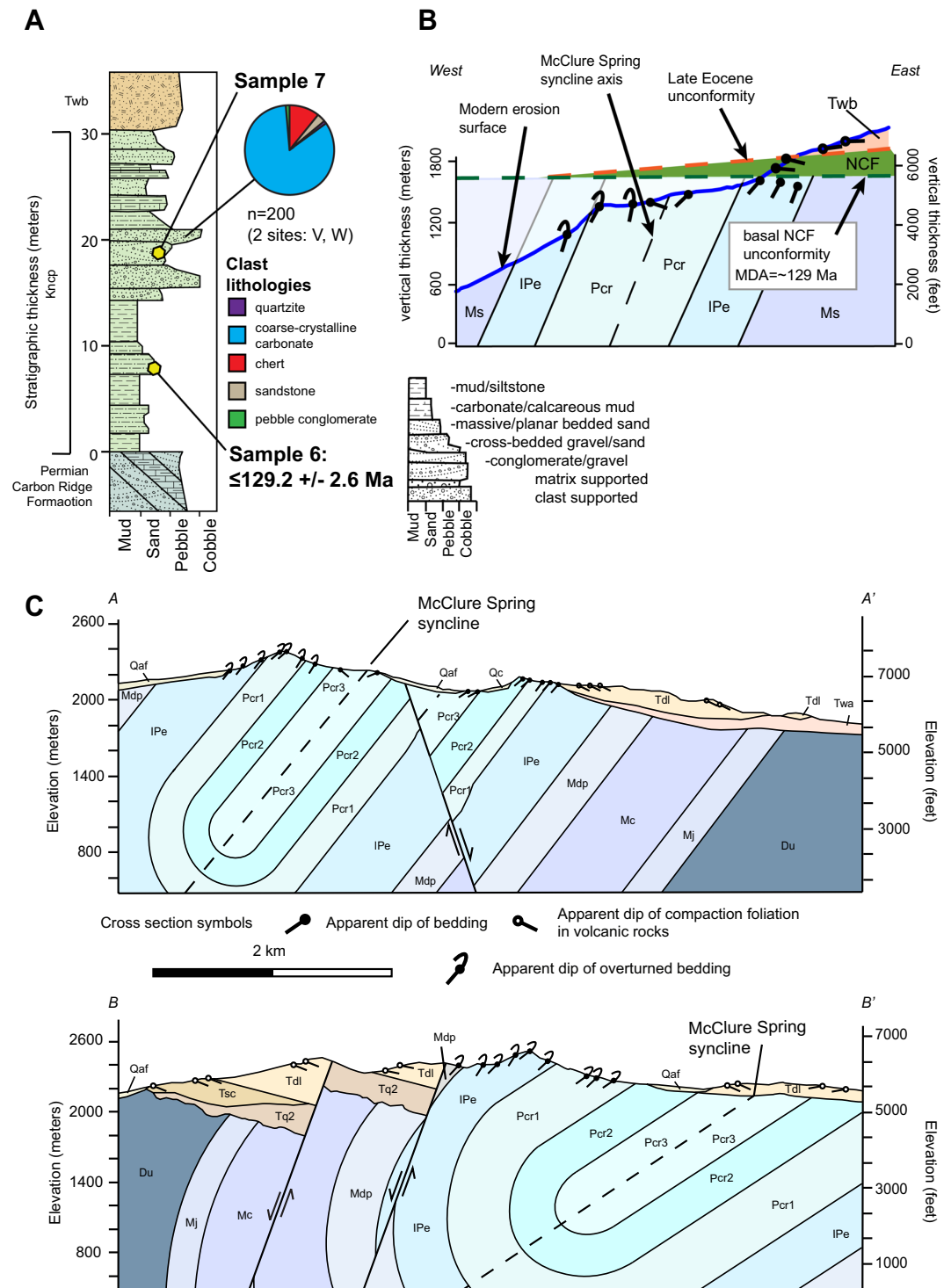


**Figure 13.** (a) Stratigraphic column of the NCF in the central Pancake Range. A combined pie chart of clast count data for the NCF is shown, as well as stratigraphic locations of U-Pb zircon geochronology samples. (b) Simplified east-west cross section through the McClure Spring syncline at the latitude of the NCF exposure ( $58^{\circ} 53' 34''$ ). Approximately  $30^{\circ}$  of eastward tilting of the basal NCF unconformity has been restored to show the orientation of the McClure Spring syncline at the time of NCF deposition. (c) Cross sections A-A' and B-B' through the central Pancake Range map area. See Figure 12 for section line locations and a guide to unit abbreviations.

present-day and pre-deformational line-lengths of a Permian bedding horizon (the Pcr2-Pcr3 contact) on our cross sections, we estimate that a minimum of  $\sim 3.2$  km of shortening was accommodated by construction of the McClure Spring syncline (Figure 13c). The axis of this km-scale, east-vergent, nearly isoclinal fold is buried beneath alluvial aprons within the hinge zone for much of the length of the map area (Figure 12).

The isolated NCF exposure in the central part of the map area exhibits a  $\sim 30^\circ$ E average dip. This NCF outcrop projects  $\sim 1$  km along-strike to the north to  $\sim 45^\circ$ W-dipping Permian rocks in the eastern, upright limb of the McClure Spring syncline (Figure 12). This defines an angular unconformity between the NCF and the underlying Permian rocks with up to  $\sim 75^\circ$  of difference in dip angle (Figure 13b).

In the northern, eastern, and southwestern parts of the map area, late Eocene to Oligocene felsic to intermediate lavas and tuffs unconformably overlie the folded Paleozoic sedimentary rocks and have an average dip of  $\sim 20^\circ$ E– $30^\circ$ E (Figures 12 and 13). The NCF lies disconformably beneath Oligocene tuff, with both units dipping  $\sim 30^\circ$ E.

#### 6.4. Tectonostratigraphic Interpretation

The field relationships exposed in the central Pancake Range map area allow bracketing the timing of construction of the McClure Spring syncline. The  $\sim 75^\circ$  angular unconformity between the east-dipping NCF and the west-dipping eastern limb of the McClure Spring syncline indicates that construction of this fold, as well as significant erosion of its eastern limb, pre-dated NCF deposition (Figure 13b). Therefore, because NCF deposition is bracketed between the Barremian ( $\sim 129$  Ma) and the end of the Cretaceous ( $\sim 66$  Ma), construction of the McClure Spring syncline must have been complete prior to  $\sim 129$ – $66$  Ma.

The disconformity observed between the NCF and overlying Oligocene tuffs indicates that there was no significant tilting of the NCF prior to the Oligocene. Therefore, the  $\sim 30^\circ$  average eastern dip observed for the NCF and the overlying Oligocene volcanic rocks can most likely be attributed to Neogene tilting accompanying regional Basin and Range extension.

### 7. Discussion

The constraints on the timing of contractional deformation and associated deposition of the NCF provided by our three map areas add to a growing body of studies that seek to understand the evolution of Mesozoic deformation in the Sevier hinterland. In the discussion below, we incorporate the new timing data from our three NCF map areas into a compilation of published timing constraints for contractional structures in the Sevier hinterland. We then use this compilation to interpret shortening in the Sevier hinterland in the broader space-time context of shortening in adjacent components of the Cordilleran retroarc thrust system, including the LFTB to the west and the Sevier fold-thrust belt to the east.

#### 7.1. Summary of Deformation Timing Constraints in the CNTB and Proximal Regions of the Sevier Hinterland

The timing of most thrust faults and folds that have been mapped in the Sevier hinterland can only be broadly bracketed between the youngest sedimentary rocks that they deform (most often Mississippian to Permian rocks, but locally as young as Triassic rocks) and the age of overlying volcanic rocks of the Great Basin ignimbrite flareup (typically ranging between late Eocene and Oligocene) (e.g., Armstrong, 1972; Gans & Miller, 1983; Long, 2012; Long & Walker, 2015; Miller & Gans, 1989; Taylor et al., 2000). Here, for simplicity, we focus on discussing only the thrust faults and folds in the Sevier hinterland that can be bracketed as Jurassic or younger and/or as Cretaceous or older. This discussion is supported by Table 1, which contains supporting details on published timing constraints, and Figure 14, which contains a map of the traces of contractional structures in a north-south corridor through central Nevada and a graph of deformation timing versus latitude. The map area of Figure 14 includes the full length of the CNTB, a region of northeastern Nevada that includes the Ruby-East Humboldt metamorphic core complex, and proximal regions of the Eastern Nevada fold belt and Sevier fold-thrust belt. Below, we discuss published timing constraints from north to south.

**Table 1**  
*Summary of Published Deformation Timing Constraints in the Sevier Hinterland in Central Nevada*

Number on Figure 14	Name of structure	Location	Data source	Timing of deformation	Explanation of supporting data
1	Prograde to peak metamorphism, burial, and nappe construction	Ruby Mountains, East Humboldt Range, Wood Hills	Camilleri & Chamberlain, 1997; Hallett & Spear, 2014, 2015; Hodges et al., 1992; McGrew et al., 2000	Late Cretaceous (~97–77 Ma)	Onset of prograde metamorphism at $96.5 \pm 8.0$ Ma (U-Pb zircon and monazite), and peak metamorphism between ~87 and 77 Ma (U-Pb zircon and monazite)
2	Independence thrust	Pequop Mountains	Zuza et al., 2020	Late Jurassic or earlier (>~160 Ma)	Thrust is cut by a lamprophyre sill that yielded $161.5 \pm 0.2$ Ma and $159.6 \pm 0.2$ Ma ( $^{40}\text{Ar}/^{39}\text{Ar}$ hornblende) ages
3	Intraformational folding in Late Jurassic Pony Trail Group volcanics	Northern Cortez Mountains	Muffler, 1964; Smith & Ketner, 1978	Late Jurassic (~164–151 Ma)	Angular unconformity between Late Jurassic volcanic unit at the base and $151 \pm 3$ Ma (K-Ar biotite) volcanic unit at the top
4	Deposition of NCF in Cortez Mountains map area	Northern Cortez Mountains	This study	Early Cretaceous (~119–110 Ma)	$119.0 \pm 1.8$ Ma tuff at base of section and $110.4 \pm 2.2$ Ma tuff at top of section (U-Pb zircon). Deposition hypothesized to be related to thrusting or folding to west/northwest of map area
5	Bald Mountain thrust faults	Bald Mountain	Nutt & Hart, 2004	Pre-Late Jurassic (>~159 Ma)	Thrust faults and related folds cut by $158.9 \pm 0.4$ Ma porphyry (U-Pb from zircon Mortensen et al., 2000; discussed in Nutt & Hart, 2004)
6	Pequop synclinorium	Currie Hills	Coats, 1987; Long & Walker, 2015; Stewart, 1980	Post-Early Jurassic	Deformation of the Early Jurassic Nugget Sandstone in the hinge zone of the fold
7	Eureka Culmination, Ratto Canyon thrust, Strahlenberg anticline, Powerline thrust, Moritz-Nager thrust, and associated NCF deposition.	Southern Diamond Mountains and northern Fish Creek Range	Di Fiori et al., 2020; Long, Henry, Muntean, Edmondo, & Cassel (2014); Long, Henry, Muntean, Edmondo, & Thomas (2014)	Early to Late Cretaceous (~114 Ma to <~99 Ma)	Age of syn-contractual deposition of the NCF in the eastern limb of the Eureka culmination. $113.7 \pm 2.3$ Ma MDA for basal NCF member, $103.0 \pm 0.7$ Ma tuff deposited in middle part of section, and $98.6 \pm 1.9$ Ma MDA for highest NCF member
8	Vanadium thrust and associated NCF deposition	Southern Fish Creek Range	This study	Early Cretaceous (~130–100 Ma)	Deposition of NCF between $129.2 \pm 1.4$ Ma (U-Pb detrital zircon MDA) and ~100 Ma (age of youngest fossils) interpreted to be related to motion on Vanadium thrust
9	Pancake thrust system	Northern Pancake Range	Carpenter et al., 1993; McDonald, 1989; Nolan et al., 1974; Long & Walker, 2015	Pre-Late Cretaceous (>~108 Ma)	Pancake thrust system is cut by $108 \pm 3$ Ma (K-Ar biotite) Puma Hill dacite stock
10	McClure Spring syncline	Central Pancake Range	This study	Post-Late Permian and pre end-Cretaceous (>~129–66 Ma)	Eastern limb of syncline was deformed and eroded prior to deposition of undeformed NCF (U-Pb zircon MDA of $129.2 \pm 1.4$ Ma, and minimum deposition age range of fossils is End Cretaceous)

**Table 1**  
*Continued*

Number on Figure 14	Name of structure	Location	Data source	Timing of deformation	Explanation of supporting data
11	Thrust faults at Mount Hamilton	Northern White Pine Range	Putney, 1985	Post-Ordovician and pre-Late Early Cretaceous (>~105–101 Ma)	Thrust faults that deform Cambrian and Ordovician rocks are cut by the $104.5 \pm 4.0$ Ma (K-Ar biotite) Seligman stock and the $101.2 \pm 3.6$ Ma (K-Ar biotite) Monte Cristo stock
12	Schofield Canyon thrust/Timber Mountain anticline	Grant Range	Fryxell, 1988; Taylor et al., 2000	Pre-Late Cretaceous (>~86 Ma)	Timber Mountain anticline is cut by Troy granite stock ( $86.4 \pm 4.6$ Ma; U-Pb zircon)
13	Rimrock thrust (and associated Rimrock-Lincoln-Freiberg thrust system)	Southern Grant Range	Bartley & Gleason, 1990; Taylor et al., 2000	Post-Pennsylvanian and pre-Late Cretaceous (>~90–98 Ma)	Thrust cuts rocks as young as Pennsylvanian and is intruded by the $90.0 \pm 2.7$ Ma to $97.9 \pm 3.0$ Ma Lincoln stock (K-Ar biotite)

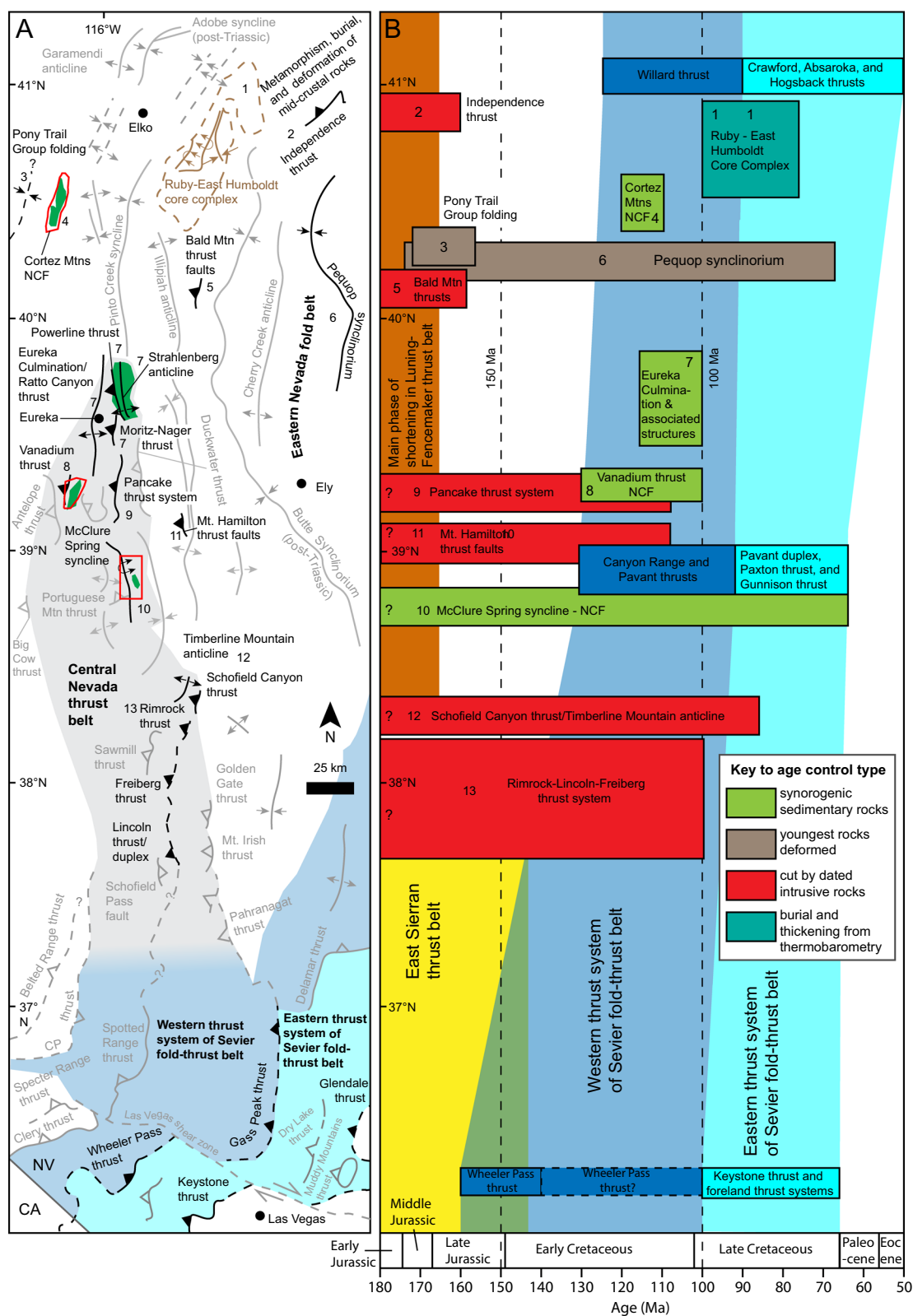
Note. Which are Graphed on Figure 14b.

Within the Ruby Mountains, East Humboldt Range, and Wood Hills in northeastern Nevada, researchers have documented evidence for metamorphism and burial of upper-crustal sedimentary protoliths to pressures up to ~6–11 kbar (~20–40 km), which has been interpreted as the consequence of Cordilleran crustal thickening (e.g., Camilleri & Chamberlain, 1997; Hallett & Spear, 2014; 2015; Henry et al., 2011; Hodges et al., 1992; McGrew, 2000). Camilleri and Chamberlain (1997) proposed that peak metamorphism was achieved by structural burial beneath a thick thrust sheet carried by the hypothesized east-vergent Windermere thrust, which can be bracketed between ~154 Ma, the timing of dike emplacement that pre-dated metamorphism, and ~84 Ma, the timing of peak metamorphism. However, because several aspects of the Windermere thrust model have been criticized by more recent studies (e.g., see arguments in Henry et al., 2011; Long, 2012; Zuza et al., 2020), we instead focus on geochronology that constrains the timing of metamorphism and burial of rocks in this region, which is bracketed between the initiation of prograde metamorphism at ~97 Ma (Hallett & Spear, 2015) and peak metamorphism between ~89 and 77 Ma (Hallett & Spear, 2014, 2015; McGrew et al., 2000). In our compilation, we interpret ~97–77 Ma as an approximate window for the timing of crustal thickening at mid-crustal levels in northeastern Nevada. This time interval also includes the ~85 Ma construction of east-vergent, recumbent nappes (including the Winchell Lake nappe) that are exposed in the East Humboldt Range (McGrew et al., 2000).

In the Pequop Mountains, the southeast-vergent Independence thrust (Camilleri & Chamberlain, 1997) has recently been interpreted by Zuza et al. (2020) to have been emplaced during the Late Jurassic, as it is cut by a ~160 Ma lamprophyre sill. However, we note that Camilleri and Chamberlain (1997) originally interpreted that the Independence thrust cuts and deforms this lamprophyre sill, which suggests a younger motion age.

In the western part of the Cortez Mountains, angular unconformities within the Late Jurassic Pony Trail Group volcanics (Figure 7) bracket intraformational folding between ~164 and ~151 Ma (Muffler, 1964). On the eastern flank of the Cortez Mountains, our U-Pb zircon ages from tuffs (Figures 4–7) bracket deposition of the NCF between ~119 and ~110 Ma. We hypothesize that NCF deposition was related to erosion of a structural high generated by Early Cretaceous folding and/or thrusting to the west of our map area, based on published paleocurrent data (Suydam, 1988) and an unroofing sequence defined by our clast composition data.

To the east of the Cortez Mountains, at Bald Mountain, several small-offset thrust faults, which deform rocks as young as Devonian, are cut by a  $158.9 \pm 0.4$  Ma (zircon U-Pb; Mortensen et al., 2000) porphyry intrusion (Nutt & Hart, 2004). To the east of Bald Mountain, the Pequop Synclinorium (Long & Walker, 2015)



deforms rocks as young as the Lower Jurassic Nugget Sandstone (Coats, 1987) near the town of Currie, indicating post-Early Jurassic construction for this fold.

In the southern Diamond Mountains, near Eureka, the NCF was deposited between  $\sim 114$  and  $\leq 99$  Ma, and is interpreted to be related to accommodation generated in the eastern limb of the Eureka culmination, a CNTB anticline that was constructed as a fault-bend fold above the east-vergent Ratto Canyon thrust (Di Fiori et al., 2020; Long, Henry, Muntean, Edmondo, & Cassel, 2014; Long, Henry, Muntean, Edmondo, & Thomas, 2014). Several east-vergent structures in the eastern limb of the Eureka culmination, including the Moritz-Nager thrust, Strahlenberg anticline, and Powerline thrust, were genetically linked to the deposition and synchronous deformation of the NCF in the southern Diamond Mountains (Di Fiori et al., 2020).

In the southern Fish Creek Range, we propose that motion on the east-vergent Vanadium thrust is the most likely scenario for generating erosion of a topographic high in the hanging wall and generating the accommodation in the footwall that the  $\sim 130$ – $100$  Ma NCF was deposited in. This interpretation is supported by our clast composition data, which are compatible with erosion of Devonian carbonates in the hanging wall of the Vanadium thrust, and published paleocurrent data (Vandervoort, 1987). To the east in the northern Pancake Range, the east-vergent Pancake thrust system, which deforms rocks as young as Mississippian, is cut by the  $\sim 108$  Ma Puma Hill dacite stock (Carpenter et al., 1993; Long & Walker, 2015; McDonald, 1989; Nolan et al., 1974), which defines pre-Late Cretaceous motion. In the central Pancake Range, our new mapping shows that the NCF overlaps the eastern limb of the McClure Spring syncline, which indicates that construction of this fold must have been completed prior to  $\sim 129$ – $66$  Ma. Additionally, in the northern White Pine Range, at Mount Hamilton, small-offset thrust faults that cut Cambrian-Ordovician rocks are cut by  $\sim 105$  and  $\sim 101$  Ma granitic stocks (K-Ar biotite; Putney, 1985).

Further to the south in the CNTB, in the Grant Range, the recumbent Timber Mountain anticline (Fryxell, 1988), which is interpreted as a fault-propagation fold that formed above the east-vergent Schofield Canyon thrust (Long et al., 2018) is intruded by the  $\sim 86$  Ma (Taylor et al., 2000) Troy granite stock, which indicates that folding was completed prior to this time. In the southern Grant Range, the Rimrock thrust, which is the northernmost segment of the east-vergent Rimrock-Lincoln-Freiberg thrust system, is cut by the  $\sim 90$ – $98$  Ma Lincoln stock, which brackets the thrust system as Late Cretaceous or older (Bartley & Gleason, 1990; Taylor et al., 2000).

## 7.2. Sevier Hinterland Deformation in the Space-Time Context of Other Cordilleran Thrust Systems

Our compilation of deformation timing constraints for the Sevier hinterland facilitates comparison to other components of the Cordilleran retroarc thrust system to the west and east. Below, we briefly discuss published timing constraints from the LFTB in western Nevada, the East Sierran thrust belt (ESTB) in southeastern California, and the Sevier fold-thrust belt in southern Nevada/western Utah. We then speculate on the role that shortening in the Sevier hinterland may have played in this broader space-time framework of Cordilleran shortening.

In western Nevada, Cordilleran deformation was dominated by the closure of a marine backarc basin, which resulted in accommodation of up to  $\sim 100$  km of shortening in the LFTB (Figures 1 and 15b) (Oldow, 1984; Wyld, 2002). The LFTB is characterized by southeast-vergent thrust faults, tight to isoclinal folds, and intense cleavage developed within Triassic sedimentary rocks (Wyld, 2002), which was accompanied by regional low-grade metamorphism (Wyld et al., 2003). The main phase of shortening within the LFTB

**Figure 14.** (a) Map of folds and thrust faults of the Sevier hinterland in central Nevada (location shown on Figure 1) (compiled from Colgan et al., 2010; Di Fiori et al., 2020; Long, 2012; Long & Walker, 2015; Taylor et al., 2000; Thorman et al., 1991). Structures that have timing constraints that narrow their motion timing as either Jurassic or younger or Cretaceous or older are highlighted in black (all structures without precise timing constraints are shown in gray). Numbers correspond to supporting studies that are compiled on Table 1. The central Nevada thrust belt is shaded gray, and the Sevier fold-thrust belt in southern Nevada is shaded blue. (b) Graph of deformation timing constraints for Sevier hinterland structures (green, gray, red, and blue-green boxes), the Luning-Fencemaker thrust belt (orange box), the East Sierran thrust belt (yellow box), and the Sevier fold-thrust belt (dark and light blue polygons) versus latitude (same latitude scale as A). Numbers correspond to supporting studies compiled on Table 1. Timing constraints for the East Sierran thrust belt (from Walker et al., 1995; Dunne & Walker, 1993; 2004), Luning-Fencemaker thrust belt (summarized in Wyld, 2002), and the western and eastern thrust systems of the Sevier fold-thrust belt are shown (from DeCelles & Coogan, 2006; Giallorenzo et al., 2018; Pujols et al., 2020; Yonkee et al., 2019); see text for discussion.

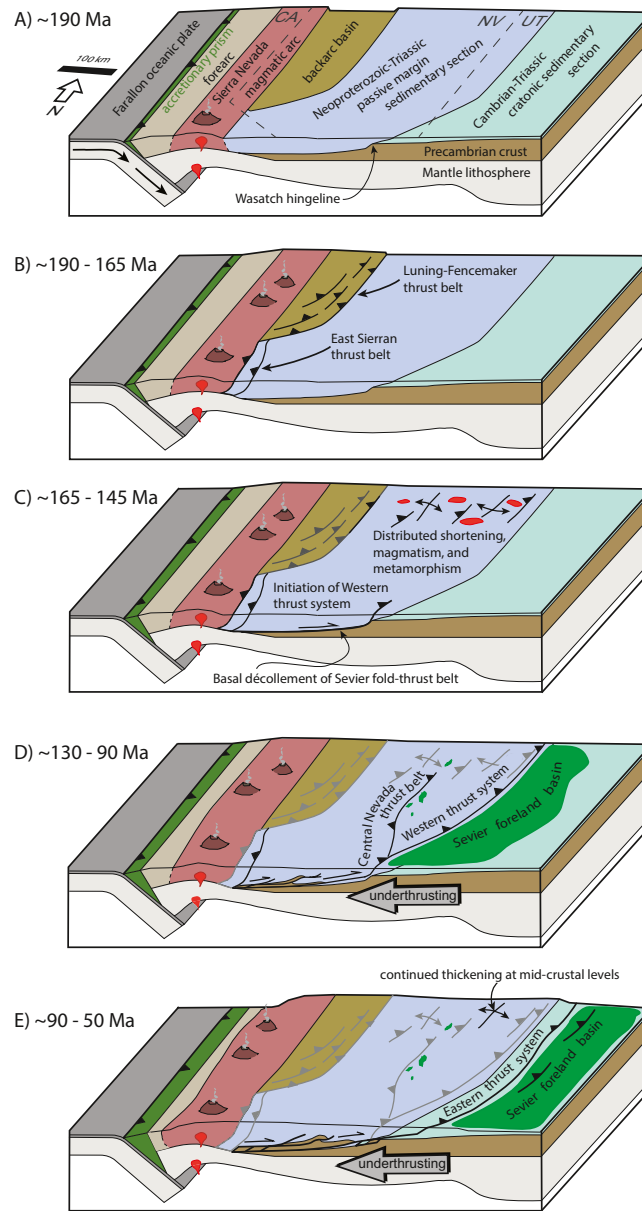


**Figure 15.** Schematic block diagrams illustrating the evolution of the Cordilleran retroarc in southeastern California, Nevada, and western Utah from the Early Jurassic to the Paleogene. The diagrams incorporate elements of Figure 6 of Yonkee and Weil (2015) and Figure 11 of Giallorenzo et al. (2018). (a) ~190 Ma, prior to any shortening in the retroarc. Geographic provinces of the Cordillera, as well as approximate locations of state borders, are labeled for reference. (b) ~190 and 165 Ma: Main phase of shortening in the Luning-Fencemaker thrust belt, which accommodated ~100 km of shortening during closure of a backarc basin, as well as initial shortening (~10 km) in the East Sierran thrust belt to the south. (c) ~165 and 145 Ma: Distributed low-magnitude shortening and associated magmatism and metamorphism in northern Nevada and western Utah, along with initiation of shortening in the western thrust system of the Sevier fold-thrust belt in southern Nevada (the Wheeler Pass thrust) and late-stage deformation within the East Sierran thrust belt. (d) ~130 and 90 Ma: Emplacement of the western thrust system of the Sevier fold-thrust belt, which initiated eastward translation of the retroarc orogenic wedge above the basal Sevier décollement (and accompanying westward underthrusting of thick, Precambrian middle-lower crust) and initial subsidence and deposition within the Sevier foreland basin. Out-of-sequence deformation in the Sevier hinterland is represented by low-magnitude shortening in the central Nevada thrust belt and associated deposition of syn-contractual sediments of the Newark Canyon Formation (green polygons). (e) ~90 and 50 Ma: Continued eastward propagation of the Sevier fold-thrust belt, represented by emplacement of the eastern thrust system. Diagram also illustrates continued deposition in the Sevier foreland basin and continued westward underthrusting as rocks above the basal Sevier décollement continued to be translated eastward. Deformation in the central Nevada thrust belt had ceased by this time but continued thickening and shortening at mid-crustal levels is recorded in northeastern Nevada (i.e., the Ruby-East Humboldt core complex).

was accomplished between the late Early and Middle Jurassic (~180–165 Ma), as bracketed by the youngest dated sedimentary rocks involved in deformation, whole rock  $^{40}\text{Ar}/^{39}\text{Ar}$  geochronology of lower greenschist-facies metasedimentary rocks, and U-Pb geochronology of undeformed intrusive rocks (Figure 15b) (Speed, 1974; Wyld, 2002; Wyld & Wright, 2000; Wyld et al., 1999). Following this, minor shortening was locally accommodated in the frontal portion of the LFTB in the Middle-Late Jurassic, prior to ~153 Ma (Figure 15c) (Elison, 1995; Elison & Speed, 1989; Wyld, 2002).

In southeastern California, at the eastern margin of the Sierra Nevada magmatic arc, the east-to-northeast-vergent ESTB accommodated up to ~10 km of shortening (Figures 1, 15b and 15c) (Dunne & Walker, 1993, 2004). Deformation in the ESTB is bracketed between the Early Jurassic (~188 Ma), the age of the youngest sedimentary rocks involved in deformation, and the latest Jurassic/earliest Cretaceous (~143–146 Ma), the crystallization age range of undeformed intrusions that cross-cut ESTB structures (Dunne & Walker, 1993, 2004; Walker et al., 1995). Shortening in the ESTB overlapped temporally with the main phase of shortening in the LFTB along-strike to the north, and the initial stages of shortening in the Sevier fold-thrust belt to the east in southern Nevada (Figures 14b, 15b and 15d).

The Sevier fold-thrust belt, which trends north-northeast through southern Nevada and western Utah (Figure 1), is estimated to have accommodated ~150–220 km of cumulative shortening (e.g., Armstrong, 1968; DeCelles & Coogan, 2006; Yonkee & Weil, 2015), making it the most significant structural component of the Cordilleran retroarc thrust system (Figures 15d and 15e). The Sevier fold-thrust belt is characterized by closely spaced, high-offset, east-vergent thrust-faults and associated folds that generally propagated in-sequence toward the east, and has been divided into a western thrust system and an eastern thrust system (e.g., DeCelles & Graham, 2015). The western thrust system consists of one thrust fault (or locally two faults; e.g., DeCelles & Coogan, 2006) that carries the ~10–15-km-thick section of Neoproterozoic to Paleozoic passive margin sedimentary rocks that were deposited to the west of the Wasatch Hingeline, and translated them as much as ~100 km eastward above a shallowly west-dipping basal décollement (Figure 15d) (e.g., DeCelles & Coogan, 2006; Yonkee et al., 1997, 2019). The eastern thrust system consists of a series of imbricate thrust faults and associated duplex systems that deform the thinner (<~5 km) section of Paleozoic-Mesozoic sedimentary rocks that was deposited to the east of the Wasatch Hingeline, and collectively accommodated ~70–100 km of shortening (Figure 15e) (e.g., DeCelles & Graham, 2015; Yonkee & Weil, 2015).

Here, we utilize recent studies at the latitudes of southern Nevada, central Utah, and northern Utah to characterize general along-strike trends in the timing of emplacement of the western and eastern thrust systems (Figure 14b). In southern Nevada (~36.5°N), the western thrust system is represented by the Wheeler Pass thrust. Initial, large-magnitude displacement on this thrust is interpreted between ~160 and ~140 Ma on the basis of bedrock cooling ages (Giallorenzo et al., 2018) (Figure 14b). In addition, the timing of prograde garnet growth in the Funeral Mountains in southeastern California requires Late Jurassic burial, which further supports this proposed timing range for motion on the Wheeler Pass thrust (Craddock et al., 2019; Hoisch et al., 2014). Based on continued cooling, motion on the Wheeler Pass thrust may have continued between ~140 and ~100 Ma, or alternatively, cooling during this time interval could reflect passive, slow erosion of topography during a period of inactivity on the thrust (Giallorenzo et al., 2018). The eastern thrust system at this latitude consists of the Keystone thrust, which underwent initial motion between ~100 and ~85 Ma, based on bedrock cooling ages (Giallorenzo et al., 2018). After ~85 Ma, deformation migrated eastward into smaller-scale foreland thrust systems that were active until ~66 Ma (e.g., Lawton et al., 1993). In west-central Utah (~39°N), the western thrust system is represented by the Canyon Range and Pavant thrusts (which both carry Neoproterozoic-Paleozoic rocks that were deposited to the west of the Wasatch Hingeline; DeCelles & Coogan, 2006), which were emplaced between ~130–125 Ma (Pujols et al., 2020) and ~93 Ma (DeCelles & Coogan, 2006) (Figure 14b). The eastern thrust system at this latitude consists of the Pavant footwall duplex, Paxton thrust, and Gunnison thrust, which were emplaced between ~93 and ~66 Ma (DeCelles & Coogan, 2006). In northern Utah (41°N), the western thrust system is represented by the Willard thrust; the onset of motion on this thrust has been interpreted at ~125 Ma on the basis of bedrock cooling ages (Figure 14b) (Yonkee et al., 2019). The eastern thrust system at this latitude consists of the Crawford, Absaroka, and Hogsback thrusts, which were emplaced between ~90 and ~50 Ma (e.g., Burtner & Nigrini, 1994; Naeser et al., 1983; Royse, 1993).

Our shortening timing compilation from central Nevada (Figure 14; Table 1), when combined with the results of studies in northeastern Nevada and northwestern Utah that lie to the east of Figure 14a (Allmendinger & Jordan, 1984; Miller & Hoisch, 1995; Thorman et al., 1991, 1992; Zuza et al., 2020), demonstrate that Late Jurassic contractional deformation, though generally of a low magnitude (i.e., limited upper-crustal shortening) and often spatially isolated (i.e., accommodated by aerally restricted structures that cannot be correlated for significant distances along-strike or across-strike), was distributed across a broad region of the northern Sevier hinterland (Figure 15c). Deformation was often spatially associated with ~155–165 Ma granitic intrusions and associated metamorphism, which defines an episode of retroarc magmatism that extended as far east as western Utah (Figure 15c) (e.g., Allmendinger & Jordan, 1984; Barton et al., 1988; Miller & Hoisch, 1995; Zuza et al., 2020). In addition, the onset of thickening at mid-crustal levels in northwestern Utah is interpreted as Late Jurassic (~150 Ma) on the basis of initial prograde metamorphism within deeply exhumed rocks now exposed in the Raft River core complex (Cruz-Urbe et al., 2015; Kelly et al., 2015). Late Jurassic deformation across the northern Sevier hinterland largely post-dated the ~180–165 Ma main phase of shortening in the LFTB to the west (Wyld, 2002), and pre-dates the Early Cretaceous (~130–125 Ma) eastward migration of the Sevier thrust front into central and northern Utah. Therefore, Late Jurassic hinterland deformation is interpreted here to represent low-magnitude, distributed crustal shortening that was contemporaneous with the ~350 km eastward propagation (estimated from the restored cross section of Long, 2019) of the deformation front between the LFTB and the Sevier fold-thrust belt between the Middle Jurassic (~165 Ma) and the Early Cretaceous (~130–125 Ma) (Figure 15c). Deformation in the Sevier hinterland was enhanced and facilitated by widespread Late Jurassic magmatism (e.g., Barton et al., 1988; Miller & Hoisch, 1995). Late Jurassic deformation in the Sevier hinterland may therefore represent internal deformation accompanying the initial stages of orogenic wedge development as the upper crust of central-eastern Nevada and western Utah was being incorporated into the Cordilleran retroarc orogenic wedge and beginning its eastward translation above the basal Sevier décollement (Figure 15c). At the latitude of southern Nevada, the migration of deformation into the Sevier fold-thrust belt was earlier (~160 Ma), overlapping in time with the distributed Late Jurassic shortening in northeastern Nevada and northwestern Utah; this has been attributed to the southward narrowing of the east-west width of the retroarc region (Giallorenzo et al., 2018).

Our compilation of deformation timing in central Nevada shows that widely distributed, low-magnitude, upper-crustal shortening also took place in the Sevier hinterland during the Cretaceous. Structures associated with NCF deposition in the northern CNTB define Early Cretaceous deformation (~130–100 Ma) (Di Fiori et al., 2020; Long, Henry, Muntean, Edmondo, & Cassel, 2014; this study), and further to the south in the CNTB deformation was completed prior to ~85 Ma (Late Cretaceous) (Taylor et al., 2000). In northeastern Nevada, metamorphism associated with significant structural burial and thickening at mid-crustal levels continued through the Late Cretaceous (~97–77 Ma) (Hallett & Spear, 2014, 2015; McGrew et al., 2000). Therefore, these data define one or more episodes of distributed Cretaceous shortening in the Sevier hinterland, which post-dated the initial propagation of deformation into the Sevier fold-thrust belt, and therefore represents out-of-sequence deformation (Figures 15d and 15e) (Di Fiori et al., 2020; Long, Henry, Muntean, Edmondo, & Cassel, 2014; Taylor et al., 2000). Shortening associated with NCF deposition generally overlapped temporally with emplacement of the western thrust system of the Sevier fold-thrust belt (Figure 14b), while Late Cretaceous thickening in northeastern Nevada overlapped with construction of the eastern thrust system. We suggest that Cretaceous deformation in the Sevier hinterland represents long-duration partitioning of contractional strain between hinterland and foreland positions in the Cordilleran retroarc wedge. Over the duration of the Cretaceous, as the Sevier fold-thrust belt was being constructed, the thick middle-lower crust of the unrifted North American craton that originally lay to the east of the Wasatch Hingeline was progressively being underthrust westward under eastern Nevada, beneath the basal Sevier décollement (Figures 15d and 15e) (Long, 2019). Cretaceous deformation in the Sevier hinterland may represent distributed shortening above the broad region of continued coupling above the décollement, which accompanied this progressive underthrusting.

## 8. Conclusions

- (1) The NCF in the Cortez Mountains was deposited between ~119 and ~110 Ma and is hypothesized to be related to thrusting or folding to the west. The NCF in the Fish Creek Range was deposited between ~130 and ~100 Ma and was likely related to motion on an east-vergent thrust fault with at least ~4 km of displacement mapped in the western part of the range. The NCF in the Pancake Range can be bracketed between ~129 and 66 Ma and post-dated construction of a km-scale, east-vergent isoclinal fold that accommodated at least ~3 km of shortening.
- (2) Late Jurassic (~165–155 Ma) contractional deformation across northeastern Nevada and northwestern Utah post-dated the main phase of shortening in the LFTB and pre-dated the initial deformation in the Sevier fold-thrust belt at this latitude. We suggest that Late Jurassic deformation in the Sevier hinterland represents distributed, low-magnitude, internal deformation that accompanied the incorporation of the upper crust of eastern Nevada and western Utah into the Cordilleran orogenic wedge as the basal décollement propagated eastward.
- (3) Cretaceous (~130–75 Ma) contractional deformation in eastern and central Nevada, including deformation associated with ~130–100 Ma deposition of the NCF, was contemporaneous with shortening in the Sevier fold-thrust belt. This defines long-duration strain partitioning between foreland and hinterland positions in the Cordilleran retroarc wedge. We suggest that hinterland deformation represents distributed, low-magnitude shortening above the broad region of continued coupling above the basal Sevier décollement, which accompanied the progressive westward underthrusting of thick North American middle-lower crust beneath Nevada.

## Data Availability Statement

Readers can access the supplementary data via the Open Science Framework (DOI <https://doi.org/10.17605/OSF.IO/WA6ER>).

## Acknowledgments

This work was funded by National Science Foundation Grant EAR-1524765 awarded to Long, Snell, and Bonde. This work was also funded by EdMAP Grant G17AC00130 awarded to Long. Additional funding includes a Graduate Student Research Grant from the Nevada Petroleum and Geothermal Society and a NASA Space Grant, both awarded to Di Fiori. The authors thank Kevin Rafferty for help and company while conducting field work. We also thank Da Wang and Charles Knaack for help with laser ablation inductively coupled plasma mass spectrometry U-Pb analyses at the WSU Geochronology Laboratory and Owen Neill, Joseph Boro, and Ross Solerno for help with the microprobe. Russell Di Fiori would also like to thank the Tomara family for letting him access their property to conduct field work. We thank Michael Wells and Adolph Yankee for constructive reviews.

## References

- Allmendinger, R. W. (1992). Fold and thrust tectonics of the western United States exclusive of the accreted terranes. In B. C. Burchfiel, P. W. Lipman, & M. L. Zoback (Eds.), *The Cordilleran orogen: Conterminous U.S.* (Vol. G-3, pp. 583–607). Geological Society of America.
- Allmendinger, R. W., Hauge, T. A., Hauser, E. C., Potter, C. J., Klemperer, S. L., Nelson, K. D., et al. (1987). Overview of the COCORP 40°N Transect, Western United States: The fabric of an orogenic belt. *Geological Society of America Bulletin*, 98, 308–319. [https://doi.org/10.1130/0016-7606\(1987\)98<308:oortnt>2.0.co;2](https://doi.org/10.1130/0016-7606(1987)98<308:oortnt>2.0.co;2)
- Allmendinger, R. W., & Jordan, T. E. (1984). Mesozoic structure of the Newfoundland mountains, Utah: Horizontal shortening and subsequent extension in the hinterland of the Sevier belt. *Geological Society of America Bulletin*, 95(11), 1280–1292. [https://doi.org/10.1130/0016-7606\(1984\)95<1280:msotnm>2.0.co;2](https://doi.org/10.1130/0016-7606(1984)95<1280:msotnm>2.0.co;2)
- Armstrong, R. L. (1968). Sevier orogenic belt in Nevada and Utah. *Geological Society of America Bulletin*, 79, 429–458. [https://doi.org/10.1130/0016-7606\(1968\)79\[429:sobina\]2.0.co;2](https://doi.org/10.1130/0016-7606(1968)79[429:sobina]2.0.co;2)
- Armstrong, R. L. (1972). Low-angle (Denudation) faults, hinterland of the Sevier orogenic belt, Eastern Nevada and Western Utah. *Geological Society of America Bulletin*, 83, 1729–1754. [https://doi.org/10.1130/0016-7606\(1972\)83\[1729:ldfhot\]2.0.co;2](https://doi.org/10.1130/0016-7606(1972)83[1729:ldfhot]2.0.co;2)
- Atwater, T. (1970). Implications of plate tectonics for the Cenozoic tectonic evolution of Western North America. *Geological Society of America Bulletin*, 81, 3513–3536. [https://doi.org/10.1130/0016-7606\(1970\)81\[3513:iopft\]2.0.co;2](https://doi.org/10.1130/0016-7606(1970)81[3513:iopft]2.0.co;2)
- Bartley, J.M., & Gleason, G.C. (1990). Tertiary normal faults superimposed on Mesozoic thrusts, Quinn Canyon and Grant Ranges, Nye County, Nevada. In Wernicke, B. P. (Ed.), *Basin and range extensional tectonics near the latitude of Las Vegas, Nevada*. Geological Society of America Memoir.
- Barton, M., Battles, D., Debout, G., Capo, R., Christensen, J., Davies, S., et al. (1988). Mesozoic Contact Metamorphism in the Western United States. In *Metamorphism and Crustal Evolution, Western Coterminous United States*, Rubey (pp. 111–178). Prentice Hall.
- Best, M. G., Barr, D. L., Christiansen, E. H., Gromme, S., Deino, A. L., & Tingey, D. G. (2009). The Great Basin Altiplano during the middle Cenozoic ignimbrite flareup: Insights from volcanic rocks. *International Geology Review*, 51, 589–633. <https://doi.org/10.1080/00206810902867690>
- Bonde, J. W., Hilton, R. P., Jackson, F. D., & Druschke, P. A. (2015). Fauna of the Newark Canyon formation (lower Cretaceous), East-Central Nevada. Presented at *Geological Society of Nevada 2015 Symposium* (pp. 139–150). Sparks, Nevada.
- Bowring, S. A., & Schmitz, M. D. (2003). High-precision U-Pb zircon geochronology and the stratigraphic record. *Reviews in Mineralogy and Geochemistry*, 53, 305–326.
- Burchfiel, B. C., Cowan, D. S., & Davis, G. A. (1992). Tectonic overview of the Cordilleran orogen in the Western United States. In B. C. Burchfiel, P. W. Lipman, & M. L. Zoback (Eds.), *The Cordilleran Orogen: Conterminous U.S.* (Vol. G-3, pp. 407–480). Geological Society of America.
- Burchfiel, B. C., & Royden, L. H. (1991). Antler orogeny: A Mediterranean-type orogeny. *Geology*, 19, 66–69. [https://doi.org/10.1130/0091-7613\(1991\)019<0066:aoamto>2.3.co;2](https://doi.org/10.1130/0091-7613(1991)019<0066:aoamto>2.3.co;2)
- Burner, R. L., & Nigrini, A. (1994). Thermochronology of the Idaho-Wyoming thrust belt during the Sevier orogeny: A new, calibrated, multiprocess thermal model. *Bulletin*, 78, 1586–1612.

- Camilleri, P. A., & Chamberlain, K. R. (1997). Mesozoic tectonics and metamorphism in the Pequop mountains and Wood Hills region, Northeast Nevada: Implications for the architecture and evolution of the Sevier orogen. *Geological Society of America Bulletin*, 109(1), 74–94. [https://doi.org/10.1130/0016-7606\(1997\)109<0074:mtamit>2.3.co;2](https://doi.org/10.1130/0016-7606(1997)109<0074:mtamit>2.3.co;2)
- Carpenter, D. G., Carpenter, J. A., Dobbs, S. W., & Stuart, C. K. (1993). Regional structural synthesis of Eureka fold-and-thrust belt, East-Central Nevada. In C. W. Gillespie (Ed.), *Structural and stratigraphic relationships of Devonian reservoir rocks, Nevada Petroleum Society, 1993 Field Conference Guidebook* (pp. 59–72).
- Cassel, E. J., Breecker, D. O., Henry, C. D., Larson, T. E., & Stockli, D. F. (2014). Profile of a paleo-orogen: High topography across the present-day basin and range from 40 to 23 Ma. *Geology*, 42, 1007–1010.
- Chang, Z., Vervoort, J. D., McClelland, W. C., & Knaack, C. (2006). U-Pb dating of zircon by LA-ICP-MS. *Geochemistry, Geophysics, Geosystems*, 7, Q05009.
- Chapman, J. B., Ducea, M. N., DeCelles, P. G., & Profeta, L. (2015). Tracking changes in crustal thickness during orogenic evolution with Sr/Y: An example from the North American Cordillera. *Geology*, 43(10), 919–922.
- Chapple, W. M. (1978). Mechanics of thin-skinned fold-and-thrust belts. *Geological Society of America Bulletin*, 89, 1189–1198.
- Coats, R. R. (1987). Geology of Elko County, Nevada. *Nevada Bureau of Mines and Geology Bulletin*, 101–112.
- Colgan, J. P., & Henry, C. D. (2009). Rapid middle Miocene collapse of the Sevier orogenic plateau in North-Central Nevada. *International Geology Review*, 51, 920–961.
- Colgan, J. P., Howard, K. A., Fleck, R. J., & Wooden, J. L. (2010). Rapid middle Miocene extension and unroofing of the Southern Ruby mountains, Nevada. *Tectonics*, 29.
- Coney, P. J., & Harms, T. J. (1984). Cordilleran metamorphic core complexes: Cenozoic extensional relics of Mesozoic compression. *Geology*, 12, 550–554.
- Coutts, D. S., Matthews, W. A., & Hubbard, S. M. (2019). Assessment of widely used methods to derive depositional ages from detrital zircon populations. *Geoscience Frontiers*, 89.
- Craddock, A. S., Hoisch, T. D., Wells, M. L., & Vervoort, J. D. (2019). Pressure-temperature-time paths from the Funeral mountains, California, reveal Jurassic retroarc underthrusting during early Sevier orogenesis. *Geological Society of America Bulletin*, 132(5–6), 1047–1065.
- Crafford, A. E. J. (2007). *Geologic map of Nevada* (Vol. 249, p. 46). U.S. Geological Survey Data Series.
- Cruz-Uribe, A. M., Hoisch, T. D., Wells, M. L., Vervoort, J. D., & Mazdab, F. (2015). Linking thermodynamic modeling, Lu-Hf geochronology, and trace elements in garnet: New P-T-t paths from the Sevier hinterland. *Journal of Metamorphic Geology*, 33(7), 763–781.
- DeCelles, P. G. (1994). Late Cretaceous-Paleocene synorogenic sedimentation and kinematic history of the Sevier thrust belt, Northeast Utah and Southwest Wyoming. *Geological Society of America Bulletin*, 106, 32–56.
- DeCelles, P. G. (2004). Late Jurassic to Eocene evolution of the Cordilleran thrust belt and foreland basin system, Western U.S.A. *American Journal of Science*, 304, 105–168.
- DeCelles, P. G., & Coogan, J. C. (2006). Regional structure and kinematic history of the Sevier fold-and-thrust belt, Central Utah. *Geological Society of America Bulletin*, 118, 841–864.
- DeCelles, P. G., & Graham, S. A. (2015). Cyclical processes in the north American Cordilleran orogenic system. *Geology*, 43(6), 499–502.
- Dickinson, W. R. (1974). Plate tectonics and sedimentation. In W. R. Dickinson (Ed.), *Tectonics and Sedimentation* (Vol. 22, pp. 1–27). Tulsa, OK: Society of Economic Paleontologists and Mineralogists (SEPM) Special Publication.
- Dickinson, W. R. (1988). Provenance and sediment dispersal in relation to paleotectonics and paleogeography of sedimentary basins. In K. L. Kleinspehn, & C. Paola (Eds.), *New perspectives in basin analysis* (pp. 3–25). Berlin: Springer-Verlag.
- Dickinson, W. R. (2002). The basin and range province as a composite extensional domain. *International Geology Review*, 44, 1–38.
- Dickinson, W. R. (2004). Evolution of the north American Cordillera. *Annual Review of Earth and Planetary Sciences*, 32, 13–44.
- Dickinson, W. R. (2006). Geotectonic evolution of the Great Basin. *Geosphere*, 2, 353–368.
- Dickinson, W. R., & Gehrels, G. E. (2009). Use of U-Pb ages of detrital zircons to infer maximum depositional ages of strata: A test against a Colorado Plateau Mesozoic database. *Earth and Planetary Science Letters*, 288, 115–125.
- Diegel, F. A. (1986). Topological constraints on imbricate thrust networks, examples from the mountain city window, Tennessee, U.S.A. *Journal of Structural Geology*, 8, 269–279.
- Di Fiori, R. V., Long, S. P., Fetrow, A., Snell, K. E., Bonde, J. A., & Vervoort, J. D. (2020). Syn-contractual deposition of the cretaceous Newark Canyon formation, Diamond mountains, Nevada: Implications for strain partitioning within the U.S. Cordillera. *Geosphere*, 61, 546–566.
- Druschke, P., Hanson, A. D., Wells, M. L., Gehrels, G. E., & Stockli, D. (2011). Paleogeographic isolation of the Cretaceous to Eocene Sevier hinterland, East-Central Nevada: Insights from U-Pb and (U-Th)/He detrital zircon ages of hinterland strata. *Geological Society of America Bulletin*, 123, 1141–1160.
- Dunne, G. C., & Walker, J. D. (1993). Age of Jurassic volcanism and tectonism, southern Owens Valley region, East-Central California. *Geological Society of America Bulletin*, 105, 1223–1230.
- Dunne, G. C., & Walker, J. D. (2004). Structure and evolution of the East Sierran thrust system, East Central California. *Tectonics*, 23.
- Elison, M. W. (1995). Causes and consequences of Jurassic magmatism in the Northern Great Basin: Implications for tectonic development. In D. M. Miller, & C. Busby (Eds.), *Jurassic magmatism and tectonics of the North American Cordillera* (Vol. 299, pp. 249–266). Geological Society of America.
- Elison, M. W., & Speed, R. C. (1989). Structural development during Flysch basin collapse: The Fencemaker allochthon, East Range, Nevada. *Journal of Structural Geology*, 11, 523–538.
- Fetrow, A. C., Snell, K. E., Di Fiori, R. V., Long, S. P., & Bonde, J. A. (2020). Syn-deformational deposition of the cretaceous Newark Canyon formation in heterogeneous palustrine, fluvial, and lacustrine environments. *Journal of Sedimentary Research*, 90(9), 1175–1197.
- Fouch, T. D., Hanley, J. M., & Forester, R. M. (1979). Preliminary correlation of Cretaceous and Paleogene lacustrine and related nonmarine sedimentary and volcanic rocks in parts of the Great basin of Nevada and Utah. In G. W. Newman, & H. D. Goode (Eds.), *Basin and range symposium and Great basin field conference* (pp. 305–312). Rocky Mountain Association of Geologists and Utah Geological Association.
- Fryxell, J. E. (1988). *Geologic Map and Description of Stratigraphy and Structure of the West-Central Grant Range, Nye County, Nevada*. Geological Society of America Map and Chart Series MCH064 (p. 16), 2 sheets, scale 1:24,000.
- Gans, P. B., & Miller, E. L. (1983). Style of mid-tertiary extension in East-Central Nevada. In K. D. Gurgel (Ed.), (Ed), *Geologic excursions in the overthrust belt and metamorphic core complexes of the intermountain region: Utah. geological and Mineral Survey Special Studies* (Vol. 59, pp. 107–160).
- Gehrels, G. E., Valencia, V., & Ruiz, J. (2008). Enhanced precision, accuracy, efficiency, and spatial resolution of U-Pb ages by laser ablation-multicollector-inductively coupled plasma-mass spectrometry. *Geochemistry, Geophysics, Geosystems*, 9, Q03017.

- Giallorenzo, M. A., Wells, M. L., Yonkee, W. A., Stockli, D. F., & Wernicke, B. P. (2018). Timing of exhumation of the Wheeler Pass thrust sheet, Southern Nevada and California: Late Jurassic to middle Cretaceous evolution of the Southern Sevier fold-and-thrust belt. *Geological Society of America Bulletin*, 130(3–4), 558–579.
- Greene, D. C. (2014). The confusion range, West-Central Utah: Fold-thrust deformation and a Western Utah thrust belt in the Sevier hinterland. *Geosphere*, 10(1), 148–169.
- Hallett, B. W., & Spear, F. S. (2014). The P-T history of anatectic pelites of the Northern East Humboldt range, Nevada: Evidence for tectonic loading, decompression, and anatexis. *Journal of Petrology*, 55(1), 3–36.
- Hallett, B. W., & Spear, F. S. (2015). Monazite, zircon, and garnet growth in migmatitic pelites as a record of metamorphism and partial melting in the East Humboldt range, Nevada. *American Mineralogist*, 100(4), 951–972.
- Heck, F. R., Elison, M. E., & Speed, R. C. (1986). Differences between foreland deformation in the Great Basin and other regions. *Geological Society of America Abstracts with Programs*, 18, 632.
- Henry, C. D., & John, D. A. (2013). Magmatism, ash-flow tuffs, and calderas of the ignimbrite flareup in the Western Nevada volcanic field, Great Basin, USA. *Geosphere*, 9, 951–1008. <https://doi.org/10.1130/GES00867.1>
- Henry, C. D., McGrew, A. J., Colgan, J. P., Snoke, A. W., & Brueseke, M. E. (2011). Timing, distribution, amount, and style of Cenozoic extension in the northern Great Basin. In J. Lee, & J. P. Evans (Eds.), *Geologic field trips to the basin and range, rocky mountains, Snake river plain, and terranes of the U.S. Cordillera* (Vol. 21, pp. 27–66). Geological Society of America Field Guide.
- Hodges, K. V., Snoke, A. W., & Hurlow, H. A. (1992). Thermal evolution of a portion of the Sevier hinterland: The Northern Ruby mountains-East Humboldt range and Wood Hills, Northeastern Nevada. *Tectonics*, 11(1), 154–164.
- Hoisch, T. D., Wells, M. L., Beyene, M. A., Styger, S., & Vervoort, J. D. (2014). Jurassic Barrovian metamorphism in a U.S. Cordilleran metamorphic core complex, Funeral mountains, California. *Geology*, 42, 399–402.
- Horton, B. K., Constenius, K. N., & DeCelles, P. G. (2004). Tectonic control on coarse-grained foreland-basin sequences: An example from the Cordilleran foreland basin, Utah. *Geology*, 32, 637–640.
- Hose, R. K. (1983). Geologic map of the Cockalorum Wash quadrangle. Eureka and Nye Counties, Nevada. United States Geological Survey Miscellaneous Investigations Series Map (I-1410, scale 1:31,680). Reno, NV: Nevada Bureau of Mines and Geology.
- Humphreys, E. D. (1995). Post-Laramide removal of the Farallon slab, Western United States. *Geology*, 23, 987–990.
- Kellogg, H. E. (1964). Cenozoic stratigraphy and structure of the southern Egan Range, Nevada. *Geological Society of America Bulletin*, 75, 949–968.
- Kelly, E. D., Hoisch, T. D., Wells, M. L., Vervoort, J. D., & Beyene, M. A. (2015). An Early Cretaceous garnet pressure-temperature path recording synconvergent burial and exhumation from the hinterland of the Sevier orogenic belt, Albion Mountains, Idaho. *Contributions to Mineralogy and Petrology*, 170, 20.
- Ketner, K. B., & Alpha, A. G. (1992). Mesozoic and tertiary rocks near Elko Nevada-Evidence for Jurassic to Eocene folding and low-angle faulting. *US Geological Survey Bulletin*, 1988-C, 13.
- Kleinhampl, F. J., & Ziony, J. L. (1985). *Geology of Northern Nye County, Nevada* (Vol. 99A, p. 171). Reno, NV: Nevada Bureau of Mines and Geology Bulletin.
- Lawton, T. F., Talling, P. J., Hobbs, R. S., Trexler, J. H., Jr, Weiss, M. P., & Burbank, D. W. (1993). Structure and stratigraphy of upper Cretaceous and Paleogene strata (North Horn formation), Eastern San Pitch mountains, Utah-Sedimentation at the front of the Sevier orogenic belt. *US Geological Survey Bulletin*, 1787, 111–133.
- Lee, J., Blackburn, T., & Johnston, S. (2017). Timing of mid-crustal ductile extension in the Northern Snake Range metamorphic core complex, Nevada: Evidence from U/Pb zircon ages. *Geosphere*, 13(2), 439–459.
- Long, S. P. (2012). Magnitudes and spatial patterns of erosional exhumation in the Sevier hinterland, Eastern Nevada and Western Utah, USA: Insights from a Paleogene paleogeologic map. *Geosphere*, 8, 881–901.
- Long, S. P. (2019). Geometry and magnitude of extension in the basin and range province (39°N), California, Nevada, and Utah, U.S.A.: Constraints from a province-scale cross section. *Geological Society of America Bulletin*, 131(1–2), 99–119.
- Long, S. P., Heizler, M. T., Thomson, S. N., Reiners, P. W., & Fryxell, J. E. (2018). Rapid Oligocene to early Miocene extension along the Grant Range detachment system, Eastern Nevada, U.S.A.: Insights from multi-part cooling histories of footwall rocks. *Tectonics*, 37.
- Long, S. P., Henry, C. D., Muntean, J. L., Edmondo, G. P., & Cassel, E. J. (2014). Early Cretaceous construction of a structural culmination, Eureka, Nevada, U.S.A.: Implications for out-of-sequence deformation in the Sevier hinterland. *Geosphere*, 10, 564–584.
- Long, S. P., Henry, C. D., Muntean, J. L., Edmondo, G. P., & Thomas, R. D. (2014). *Geologic map of the southern part of the Eureka mining district, and surrounding areas of the Fish Creek range, mountain Boy Range, and Diamond mountains, Eureka and White Pine Counties, Nevada* (Map 183, scale 1:24,000, 2 plates). Reno, NV: Nevada Bureau of Mines and Geology.
- Long, S. P., & Walker, J. P. (2015). Geometry and kinematics of the Grant Range brittle detachment system, eastern Nevada, U.S.A.: An end-member style of upper-crustal extension. *Tectonics*, 34, 1837–1862.
- Ludwig, K. R. (2008). *User's manual for Isoplot 3.6: Geochronological toolkit for Microsoft* (vol. 4, p. 78). Berkeley Geochronology Center, Special Publication.
- McDonald, S. F. (1989). *Geology, Pogues Station Quadrangle, White Pine and Nye Counties, Nevada* (M.S. thesis). San Diego, CA: San Diego State University.
- McGrew, A. J., Peters, M. T., & Wright, J. E. (2000). Thermobarometric constraints on the tectonothermal evolution of the East Humboldt range metamorphic core complex, Nevada. *Geological Society of America Bulletin*, 112(1), 45–60.
- McQuarrie, N., & DeCelles, P. G. (2001). Geometry and structural evolution of the Central Andean backthrust belt, Bolivia. *Tectonics*, 17, 203–220.
- Miller, D., & Hoisch, T. (1995). Jurassic tectonics of Northern Nevada and Northwestern Utah from the perspective of barometric studies. *Geological Society of America Special Paper*, 299, 267–294.
- Miller, E. L., & Gans, P. B. (1989). Cretaceous crustal structure and metamorphism in the hinterland of the Sevier thrust belt, Western US Cordillera. *Geology*, 17(1), 59–62.
- Miller, E. L., Gans, P. B., Wright, J. E., & Sutter, J. F. (1988). Metamorphic history of the east-central Basin and Range Province: Tectonic setting and relationship to magmatism. In W. G., Ernst (Ed.), *Metamorphism and Crustal Evolution, Western Conterminous United States, Rubey* (Vol. 7). Englewood Cliffs, NJ: Prentice-Hall.
- Morley, C. K. (1988). Out-of-sequence thrusts. *Tectonics*, 7(3), 539–561.
- Mortensen, J. K., Thompson, J. F. H., & Tosdal, R. M. (2000). U-Pb age constraints on magmatism and mineralization in the northern Great Basin, Nevada. In J. K. Cluer, J. G. Price, E. M. Struhsacker, R. F. Hardyman, C. L. Morris (Eds.), *Geology and Ore Deposits 2000: The Great Basin and Beyond. Geological Society of Nevada Symposium Proceedings, Reno, May 15–18, 2000* (pp. 419–438).
- Muffler, L. J. P. (1964). *Geology of the Frenchie Creek quadrangle, North-Central Nevada. U.S. Geological Survey Bulletin*, 1179, 99.

- Naeser, C. W., Bryant, B., Crittenden, M. D., Jr., & Sorensen, M. L. (1983). Fission track ages of apatite in the Wasatch mountains, Utah, an uplift study. In D. M. Miller, R. Todd, & K. A. Howard (Eds.), *Tectonic and stratigraphic studies in the eastern Great Basin* (Vol. 157, pp. 29–36). Geological Society of America Memoirs.
- Nolan, T. B. (1962). *The Eureka mining district, Nevada. US Geological Survey Professional Paper 406* (p. 78). US Government Printing Office.
- Nolan, T. B., Merriam, C. W., & Blake, M. C., Jr. (1974). *Geologic map of the Pinto Summit quadrangle, Eureka and White Pine Counties, Nevada*. U.S. Geological Survey Miscellaneous Investigations Series Map (I-793, scale 1: 31,680, 14, 2 plates). Washington: U.S. Government Printing Office.
- Nolan, T. B., Merriam, C. W., & Brew, D. A. (1971). *Geologic map of the Eureka quadrangle, Eureka and white pine Counties, Nevada*. U.S. Geological Survey Miscellaneous Investigations Series Map (I-612, scale 1: 31,680, 8, 2 plates). U.S. Government Printing Office.
- Nolan, T. B., Merriam, C. W., & Williams, J. S. (1956). *The stratigraphic section in the vicinity of Eureka, Nevada. U.S. Geological Survey Professional Paper 276* (p. 77). U.S. Government Printing Office.
- Nutt, C. J., & Hart, K. S. (2004). *Geologic map of the Big Bald mountain quadrangle and part of the Tognini Spring quadrangle, white pine county, Nevada* (Map 145, scale 1:24,000, 1 plate). Nevada Bureau of Mines and Geology.
- Oldow, J. S. (1984). Evolution of a late Mesozoic back-arc fold and thrust belt, Northwestern Great Basin, U.S.A. *Tectonophysics*, 102, 245–274.
- Perry, W. J., & Dixon, G. L. (1993). Structure and time of deformation in the Central Pancake Range, a geologic reconnaissance. In C. W. Gillespie (Ed.), *Structural and stratigraphic relationships of Devonian Reservoir Rocks, East-Central Nevada, Nevada Petroleum Society 1993 fieldtrip Guidebook* (pp. 123–132). Reno, NV: Nevada Bureau of Mines and Geology.
- Poole, F. G., Stewart, J. H., Palmer, A. R., Sandberg, C. A., Madrid, R. J., Ross, R. J., Jr, et al. (1992). Latest Precambrian to latest Devonian time; development of a continental margin. In B. C. Burchfiel, P. W. Lipman, & M. L. Zoback (Eds.), *The Cordilleran orogen: Conterminous U.S.* (Vol. G-3, pp. 9–56). Boulder, CO: Geological Society of America.
- Pujols, E. J., Stockli, D. F., Constenius, K. N., & Horton, B. K. (2020). Thermochronological and geochronological constraints on Late Cretaceous unroofing and proximal sedimentation in the Sevier orogenic belt, Utah. *Tectonics*, 39.
- Putney, T. R. (1985). *Geology, geochemistry, and alteration of the Seligman and Monte Cristo Stocks, White Pine mining district, White Pine County, Nevada* (M.S. thesis) (Vol. 164). Reno, NV: University of Nevada.
- Royse, F. (1993). An overview of the geologic structure of the thrust belt in Wyoming, Northern Utah, and Eastern Idaho. In A. W. Snoke, J. R. Steidtmann, & S. M. Roberts (Eds.), *Geology of Wyoming* (Vol. 5, pp. 272–311). Geological Survey of Wyoming Memoir.
- Royse, F., Jr, Warner, M. A., & Reese, D. L. (1975). Thrust belt structural geometry and related stratigraphic problems Wyoming-Idaho-Northern Utah. In D. W. Bolyard (Ed.), *Deep drilling frontiers of the central Rocky Mountains* (pp. 41–54). Rocky Mountain Association of Geologists.
- Schoene, B. (2014). U-Th-Pb geochronology. In H. D. Holland, & K. K. Turekian (Eds.), *The Crust, treatise on Geochemistry* (2nd ed., Vol. 4, pp. 341–378). Oxford: Elsevier.
- Smith, F. R., Jr, & Ketner, K. B. (1976). *Stratigraphy of Post-Paleozoic rocks and summary of resources in the Carlin-Piñon range area, Nevada*. U.S. Geological Survey Professional Paper 867-B.
- Smith, F. R., Jr, & Ketner, K. B. (1977). *Tectonic events since early Paleozoic in the Carlin-Pinon range area, Nevada*. U.S. Geological Survey Professional Paper 867-C.
- Smith, F. R., Jr, & Ketner, K. B. (1978). *Geologic map of the Carlin-Pinon range area, Elko and Eureka Counties, Nevada*. U.S. Geological Survey Miscellaneous Investigations Map (I-1028, scale 1:62,500). Reno, NV: Nevada Bureau of Mines and Geology.
- Smith, M. E., Carroll, A. R., Jicha, B. J., Cassel, E. J., & Scott, J. J. (2014). Paleogeographic record of Eocene Farallon slab rollback beneath Western North America. *Geology*, 42.
- Snell, K. E., Koch, P. L., Druschke, P., Foreman, B. Z., & Eiler, J. M. (2014). High elevation of the ‘Nevadaplano’ during the Late Cretaceous. *Earth and Planetary Science Letters*, 386, 52–63.
- Speed, R. C. (1974). Evaporite-carbonate rocks of the Jurassic Lovelock formation, West Humboldt range, Nevada. *Geological Society of America Bulletin*, 85, 105–118.
- Speed, R. C. (1983). Evolution of the sialic margin in the Central-Western United States. In J. S. Watkins, & C. L. Drake (Eds.), *Studies in continental margin Geology* (Vol. 34, pp. 457–468). Tulsa, OK: American association of Petroleum Geologists Memoir.
- Speed, R. C., Elison, M. W., & Heck, R. R. (1988). Phanerozoic tectonic evolution of the Great Basin. In W. G. Ernst (Ed.), *Metamorphism and crustal evolution of the Western United States, Ruby* (Vol. 7, pp. 572–605). Prentice-Hall.
- Stewart, J. H. (1980). *Geology of Nevada: A discussion to accompany the geologic map of Nevada*. Nevada Bureau of Mines and Geology Special Publication.
- Stewart, J. H., & Carlson, J. E. (1978). *Geologic map of Nevada*. U.S. Geological Survey (scale 1:500,000). Reno, NV: Nevada Bureau of Mines and Geology.
- Stewart, J. H., & Poole, F. G. (1974). Lower Paleozoic and uppermost Precambrian Cordilleran miogeocline, Great Basin, Western United States. In W. R. Dickinson (Ed.), *Tectonics and sedimentation* (Vol. 22, pp. 28–57). Tulsa, OK: SEPM Society for Sedimentary Geology-Special Publication.
- Sturmer, D. M., Trexler, J. H., Jr, & Cashman, P. H. (2018). Tectonic analysis of the Pennsylvanian Ely-Bird spring basin: Late Paleozoic tectonism on the Southwestern Laurentia margin and the distal limit of the ancestral rocky mountains. *Tectonics*, 37, 604–620.
- Suydam, J. D. (1988). Sedimentology, provenance, and Paleotectonic Significance of the Cretaceous Newark Canyon formation, Cortez mountains, Nevada (M.S. thesis). Bozeman, MT: Montana State University.
- Taylor, W. J., Bartley, J. M., Fryxell, J. E., Schmitt, J., & Vandervoort, D. S. (1993). Mesozoic central Nevada thrust belt. In M. M. Lahren, J. H. Trexler, & C. Spinosa (Eds.), *Crustal evolution of the Great Basin and the Sierra Nevada* (pp. 57–96). Geological Society of America.
- Taylor, W. J., Bartley, J. M., Martin, M. W., Geissman, J. W., Walker, J. D., Armstrong, P. A., & Fryxell, J. E. (2000). Relations between hinterland and foreland shortening: Sevier orogeny, Central North American Cordillera. *Tectonics*, 19, 1124–1143.
- Thorman, C. H., Ketner, K. B., Brooks, W. E., Snee, L. W., & Zimmermann, R. A. (1991). Late Mesozoic-Cenozoic tectonics in Northeastern Nevada. In G. I. Raines, R. E. Lisle, R. W. Schafer, & W. H. Wilkinson (Eds.), *Geology and ore deposits of the Great Basin, Symposium Proceedings* (pp. 25–45). The Geological Society of Nevada.
- Thorman, C. H., Ketner, K. B., & Peterson, F. (1992). The Middle to Late Jurassic Elko orogeny in Eastern Nevada and Western Utah. *Geological Society of America Abstracts with Programs*, 24, 66.
- Trexler, J. H., Jr, Cashman, P. H., Snyder, W. S., & Davydov, V. I. (2004). Late Paleozoic tectonism in Nevada: Timing, kinematics, and tectonic significance. *Geological Society of America Bulletin*, 116(5), 525–538.

- Vandervoort, D. S. (1987). Sedimentology, provenance, and tectonic implications of the cretaceous Newark Canyon formation, East-Central Nevada (M.S. thesis). Bozeman, MT: Montana State University.
- Vandervoort, D. S., & Schmitt, J. G. (1990). Cretaceous to early Tertiary paleogeography in the hinterland of the Sevier thrust belt, East-Central Nevada. *Geology*, 18, 567–570.
- Villien, A., & Kligfield, R. M. (1986). Thrusting and synorogenic sedimentation in Central Utah. In J. A. Peterson, (Ed.), *Paleotectonics and sedimentation in the Rocky mountain region, United States* (Vol. 41, pp. 281–308). American Association of Petroleum Geologists Memoir.
- Walker, J. D., Burchfiel, B. C., & Davis, G. A. (1995). New age controls on initiation and timing of foreland belt thrusting in the Clark mountains, Southern California. *Geological Society of America Bulletin*, 107, 742–750.
- Wells, M. L., Dallmeyer, R. D., & Allmendinger, R. W. (1990). Late Cretaceous extension in the hinterland of the Sevier thrust belt, North-western Utah and Southern Idaho. *Geology*, 18(10), 929–933.
- Wernicke, B. (1992). Cenozoic extensional tectonics of the U.S. Cordillera. In B. C. Burchfiel, P. W. Lipman, & M. L. Zoback (Eds.), *The Cordilleran orogen: Conterminous U.S.* (Vol. G-3, pp. 553–581). Geologic Society of America.
- Wyld, S. J. (2002). Structural evolution of a Mesozoic backarc fold-and-thrust belt in the U.S. Cordillera: New evidence from Northern Nevada. *Geological Society of America Bulletin*, 114, 1452–1468.
- Wyld, S. J., Copeland, P., & Rogers, J. W. (1999).  $^{40}\text{Ar}/^{39}\text{Ar}$  whole rock phyllite ages from the Mesozoic Luning-Fencemaker thrust belt of Central Nevada. *Eos, Transactions, American Geophysical Union*, 80(46), F977.
- Wyld, S. J., Rogers, J. W., & Copeland (2003). Metamorphic evolution of the Luning- Fencemaker fold-thrust belt, Nevada: Illite crystallinity, metamorphic petrology, and  $^{40}\text{Ar}/^{39}\text{Ar}$  geochronology. *Geology*, 111, 17–38.
- Wyld, S. J., & Wright, J. E. (2000). Timing of deformation in the Mesozoic Luning-Fencemaker fold-thrust belt, Nevada. *Geological Society of America Abstracts with Programs*, 32(7), A169–A170.
- Yonkee, W. A., DeCelles, P. G., & Coogan, J. C. (1997). Kinematics and synorogenic sedimentation of the eastern frontal part of the Sevier orogenic wedge, Northern Utah. In P. K. Link, & B. J. Kowallis (Eds.), *Proterozoic to recent stratigraphy, tectonics, and volcanology, Utah, Nevada, Southern Idaho and Central Mexico* (Vol. 42, pp. 355–380). Brigham Young University Geology Studies.
- Yonkee, W. A., Eleogram, B., Wells, M. L., Stockli, D. F., Kelley, S., & Barber, D. E. (2019). Fault slip and exhumation history of the Willard thrust sheet, Sevier fold-thrust belt, Utah: Relations to wedge propagation, hinterland uplift, and foreland basin sedimentation. *Tectonics*, 38, 2850–2893.
- Yonkee, W. A., & Weil, A. B. (2015). Tectonic evolution of the Sevier and Laramide belts within the North American Cordillera orogenic system. *Earth-Science Reviews*, 150, 531–593.
- Zuza, A. V., Thorman, C. H., Henry, C. D., Levy, D. A., Dee, S., Long, S. P., et al. (2020). Pulsed Mesozoic deformation in the Cordilleran hinterland and evolution of the Nevadaplano: Insights from the Pequop mountains, NE Nevada. *Lithosphere*, 2020(1).